https://doi.org/10.5194/egusphere-2026-819
Preprint. Discussion started: 11 March 2026


# Sediment storage and routing in bedrock canyons

Chloe B.A. Ross[1,2], Julia C. Carr[1], Jeff E. Larimer[1], Max Hurson[1,3], Leonard S. Sklar[1], Morgan Wright[1], Nick Viner[4], Jeremy G. Venditti[1]

[1]School of Environmental Science, Simon Fraser University, Burnaby, V5A 1S6, Canada
[2]Department of Earth Sciences, Simon Fraser University, Burnaby, V5A 1S6, Canada
[3]Department of Geography, University of British Columbia, Vancouver, V6T 1Z4, Canada
[4]Hakai Institute, Victoria, V8W 1T4, Canada

**Correspondence:** Chloe B.A. Ross (chloe_ross@sfu.ca)

**Abstract.** Bedrock river bathymetry is dynamic, with incision rates dependent on sediment cover, supply, and mobility in the channel. However, the scale and fluctuation of this dynamic sediment storage is not well understood, particularly in large bedrock rivers where the bed is not visible at low flows. We used repeat, high resolution, multibeam bathymetric surveys from 2021-2023 to characterize bed and bank topography in nine bedrock canyons that are representative of a wide range of width, depth, slope, and velocity observed through the 375 km long Fraser Canyon in British Columbia. Change in elevation as high as 15 m is identified between surveys. We characterize patches of contiguous change to measure changes in sediment storage volume. Our observations reveal that channel morphology determines where storage occurs. We find that sediment is 'staged' through canyons, initially being deposited in a canyon near a sediment supply site, then moving downstream as the initial deposit declines. Substantial changes in storage volume occur without substantial changes in patch footprint. These findings provide key context for interpreting the reach-scale structure of bedrock erosion, the long-term evolution of mountain river networks, and the moderation of sediment delivery to lowland environments.

## 1 Introduction

The propagation of climatic and tectonic signals through river networks is controlled by reaches where erosion-resistant bedrock dominates the bed and banks (Whipple et al., 2013). It is here that the rate of landscape evolution is limited by the rate of bedrock fluvial incision (Rennie et al., 2018; Turowski et al., 2008; Venditti et al., 2020b; Whipple and Meade, 2004; Wohl, 2015) because bedrock-bound reaches present hard points that must be incised along the river profile and determine the base level of upstream landscapes (Venditti, 2026). Local incision processes are controlled by hydraulic and sediment conditions at the bed (Chatanantavet and Parker, 2008; Lamb et al., 2008, 2015; Larsen and Lamb, 2016; Li et al., 2020, 2021, 2023; Sklar and Dietrich, 2004; Turowski et al., 2007, 2008; Yanites, 2018; Zhang et al., 2015). Bedrock is eroded by abrasion and plucking, with abrasion dominating in regions with competent massive bedrock (Lamb et al., 2015). Plucking is important where rock is highly jointed, but abrasion still plays a key role in increasing the mobility of large plucked rocks by reducing their size through battering (Chatanantavet and Parker, 2008). Sediment plays a critical role in incision because sediment cover

https://doi.org/10.5194/egusphere-2026-819
Preprint. Discussion started: 11 March 2026


can shield the bed from erosion, yet also acts as tools that cause abrasion and batter rock where it is exposed (Sklar and Dietrich, 2004). In general, low sediment cover results in the dominance of vertical incision, whereas high cover shields the bed and causes deflection of particles into the banks which widens the channel (Finnegan et al., 2007; Fuller et al., 2016; Li et al., 2020, 2021, 2022, 2023).

Early models for predicting sediment cover in bedrock rivers were based on the assumption that the fraction of bedrock bed covered by transient deposits of alluvium should vary with the rate of coarse sediment supply relative to the bedload sediment transport capacity (Gasparini et al., 2007; Sklar and Dietrich, 1998, 2004; Turowski et al., 2007). This assumption is supported by results of laboratory experiments that used planar bedrock surfaces and uniform sediment grain sizes (Chatanantavet and Parker, 2008; Larimer et al., 2021; Scheingross et al., 2014, 2017; Scheingross and Lamb, 2016; Sklar and Dietrich, 2001). However, numerous field studies have shown that spatial patterns of sediment storage within bedrock channels are strongly influenced by the local topography of underlying bedrock (Beer et al., 2017; Goode and Wohl, 2010; Turowski et al., 2008). As a result, more recent cover models include bedrock roughness as a controlling variable, and treat cover as a function of the thickness of sediment storage relative to a characteristic roughness height (Inoue et al., 2014; Johnson, 2014; Shobe et al., 2017; Zhang et al., 2015). In this framework, sediment cover and storage are linked, and depend on the temporal sequence of sediment supply events and the local feedbacks among sediment storage, bed topography, flow hydraulics, and sediment transport (Buechel et al., 2022; Hodge et al., 2011; Hodge and Buechel, 2022; Hodge and Hoey, 2016). Sediment supply, in turn, depends on the lithologic, climatic, and geomorphic factors that control sediment production in upstream catchments (Sklar, 2024), and by episodic events that deliver coarse sediment to the channel (e.g. debris flows, landslides, rock falls). The timing of hillslope input events relative to peak flow influences whether an erosive or depositional signal will propagate (DeLisle and Yanites, 2023; Lague, 2010; Turowski et al., 2013), while channel morphology and the sediment storage legacy of previous events will influence how those signals translate or disperse downstream.

In active orogens, bedrock-bound reaches are often characteristically narrow, deeply incised, and relatively straight channels (e.g. Baker et al., 1988; Bretz, 1924; Ouimet et al., 2008; Rennie et al., 2018) that follow structural weakness in the rock (e.g. Curran et al., 2023). These channels typically alternate with comparatively wide and shallow unconstrained non-bedrock reaches (Dolan et al., 1978; Rennie et al., 2018; Venditti et al., 2020a, b; Whipple et al., 2013; Wohl, 2015; Wright et al., 2024). Both experimental and field studies of narrow bedrock canyons have shown that sediment cover and morphology are interrelated (e.g. Cao et al., 2022; Cook et al., 2013; Hurson et al., 2022; Finnegan et al., 2010; Johnson and Whipple, 2010; Kusack et al., 2024). While bedrock channels can have planform morphologies similar to alluvial channels (e.g. meandering, anabranching, straight) (e.g. Wohl, 1998; Wohl and Merritt, 2001), there are also morphologies unique to bedrock-bound channels where the banks are bedrock and the bed is only intermittently covered by sediment (Venditti, 2026). These include (1) constriction-pool-widenings (CPWs), (2) rapids, and (3) overfalls (Figure 1).

https://doi.org/10.5194/egusphere-2026-819
Preprint. Discussion started: 11 March 2026


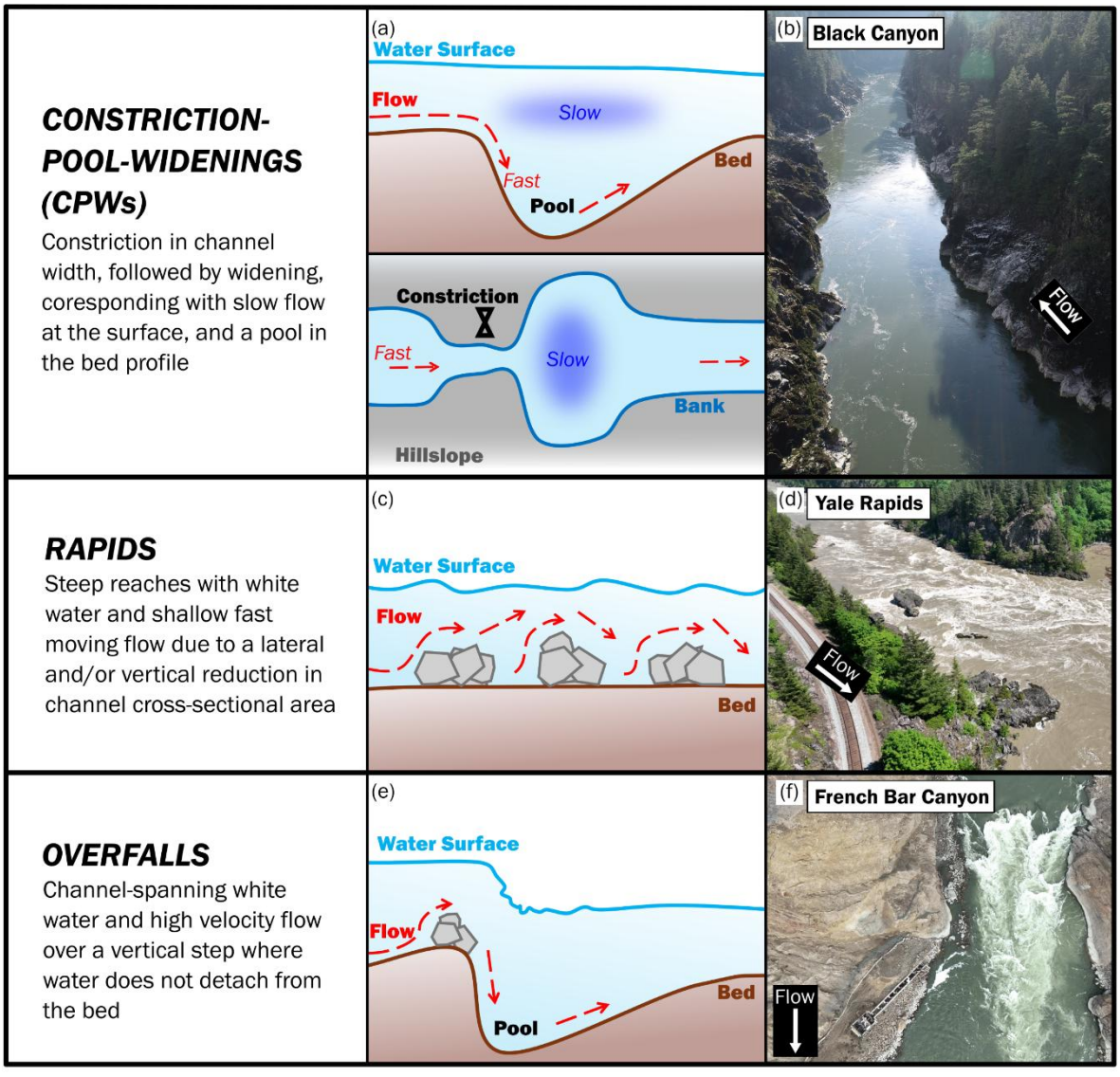


**Figure 1. Morphology and flow structure in bedrock-bound channels (Wright et al., 2024; Venditti, 2026). Photos of each morphology are from the Fraser River, British Columbia, Canada.**

Constriction-pool-widenings (CPWs) are places where a local constriction in channel width causes a deep pool to form within and downstream of the constriction, followed by a channel widening (Venditti et al., 2014, 2020a; Wright et al., 2024). This morphological sequence develops where channel constrictions force plunging flows that cause a velocity inversion (high velocity at the bed, and low velocity at the surface) (Hunt et al., 2018; Hurson et al., 2022; Hurson et al., 2025; Li et al., 2022; Venditti et al., 2014). Plunging flows form due to a backwater developing upstream of the narrowing, which causes flow to spill through the constriction, and plunge towards the bed in the centre of the channel (Cao et al., 2022; Hunt et al., 2018;

https://doi.org/10.5194/egusphere-2026-819
Preprint. Discussion started: 11 March 2026


Hurson et al., 2022, 2025; Venditti et al., 2014). These plunging flows scour the bed and carve a deep pool downstream of the constriction (Cao et al., 2022; Kusack et al., 2024; Hurson et al., 2022; 2025). Plunging flows are maintained through the pool by a secondary circulation that brings slow moving fluid from the bed to the water surface along the channel margins (Hurson et al., 2022; Venditti et al., 2014). The secondary circulation as well as particle deflections off sediment deposits drive sediment into the canyon walls downstream of the constriction, resulting in lateral erosion and widening (Kusack et al., 2024; Li et al., 2020, 2021, 2022, 2023; Venditti et al., 2014). Previous work on CPWs has shown variation in sediment cover where it can be entrained at high flows and subsequently redeposited at low flows (Hurson et al., 2022). There is also evidence of coherent variation in sediment cover with patches forming in the bottom of pools and on the pool exit slopes at low flows (Hurson et al., 2022; 2025; Kusack et al., 2024).

Rapids are typically steep reaches where relatively shallow flow travels over bedrock steps and/or boulders with visible whitewater at the surface (Leopold, 1969). They can occur in channels where tributaries and other lateral sediment inputs deliver particles too large to be easily moved by annual flows (Dolan et al., 1978; Graf, 1979; Hammack and Wohl, 1996; Kieffer, 1985; Larsen et al., 2004; Webb et al., 1988). These inputs may develop debris fans, which create a fan-eddy complex (Schmidt, 1990) consisting of a backwater upstream of the constriction, accelerated flow past the fan deposit, a horizontal recirculation eddy in the downstream widening, and a gravel or sand bar where sediment supply is abundant (Alvarez et al., 2017; Alvarez and Grams, 2021; Grams et al., 2007; Mueller et al., 2018; Schmidt, 1990; Schmidt and Rubin, 1995). Rapids also may occur without lateral sediment inputs where bedrock or boulders force a lateral constriction or a cross-channel sill (Venditti et al., 2020a; Wright et al., 2024). Breaking surface waves that produce highly aerated white water occur at rapids (Kieffer, 1985, 1988, 1989). Bolder and bedrock enforced rapids may span all or only part of the channel width (Wright et al., 2024) and need not be coupled with a channel widening or lateral recirculation eddy (Venditti, 2026).

Overfalls are like rapids in that they occur at locations with bedrock or boulder steps, however, these steps typically span the entire width of the channel (Wright et al., 2024). The flow structure is similar to a waterfall but without flow detachment from the boundary and freefall through the air (Venditti, 2026). Overfalls may also occur where the channel is severely constricted. Overfalls have significant water surface elevation change (several meters) that results in an impinging jet and a plunge pool (Hurson et al., in review). This vertical drop produces transcritical or supercritical flow over the bedrock steps, and large standing and breaking waves as the flow transitions back to subcritical flow downstream of the steps (Kieffer, 1985; Magirl et al., 2009). Notable examples of overfalls are the one created by the 2018 Big Bar Landslide as well as at Bridge River Rapid in the Fraser River (Venditti, 2026).

Differentiating the impacts of different bedrock-bound channel morphologies and flow structures on sediment storage and cover is challenging because the location and magnitude of sediment erosion and deposition can vary with both morphology and supply events. Here we explore the variation in sediment storage in large bedrock canyons following a major sediment

https://doi.org/10.5194/egusphere-2026-819
Preprint. Discussion started: 11 March 2026


supply event. We aim to understand how channel morphology and sediment supply influence sediment dynamics in CPWs, rapids, and overfalls. We use high-resolution, repeat bathymetric surveys to explore the variation in bed topography caused by changes in sediment storage in a large bedrock canyon system. We measure changes in sediment volume between repeat surveys and identify regional patterns in relation to channel morphology and following a major sediment supply event that delivered sediment to the channel where hillslope-channel connectivity is high. Our research questions are: (1) How do sediment storage and cover vary spatially and temporally in a large bedrock river; (2) Do patterns of sediment storage and routing vary with channel morphology; and (3) How does sediment storage vary with changes in discharge following a high sediment input event?

## 2 Methodology

### 2.1 Study Area

The Fraser River drains ~232,000 km$^2$ of British Columbia, Canada, flowing ~1375 km from Mount Robson to the Pacific Ocean (Figure 2). Between Soda Creek and Yale is a 375 km bedrock influenced reach, colloquially referred to as the Fraser Canyon, which is comprised of a series of bedrock canyons that are conspicuously narrow and deeply incised, interspersed with wider reaches without obvious bedrock exposure (Venditti et al., 2020a). The banks within the Fraser Canyon are ~26% bedrock-bound (both sides bedrock), ~29% bedrock-constrained (one side bedrock), and ~45% non-bedrock (Rennie et al., 2018). The non-bedrock reaches are a mix of alluvial material, glaciofluvial terraces, colluvial deposits composed of boulders kinetically sieved and washed from the glaciofluvial terraces, colluvial bases of talus slopes, and debris flow deposits washed of finer materials (Curran et al., 2023; Rennie et al., 2018; Venditti et al., 2014; Wright et al., 2022). The Fraser River is a freshet dominated system that experiences the highest flow from late spring to early summer (May to June) during snowmelt, with flow then receding into late summer, followed by low flows in the fall and winter when the snowpack rebuilds (September to April) (Figure 3). A gauging station near the exit of the Fraser Canyon in Hope, British Columbia (Water Survey of Canada Gauge 08MF005), has a mean annual peak flow of 8420 m$^3$/s, a mean annual flow of 2700 m$^3$/s, and a baseflow of ~1000 m$^3$/s (Hurson et al., 2022).

https://doi.org/10.5194/egusphere-2026-819
Preprint. Discussion started: 11 March 2026


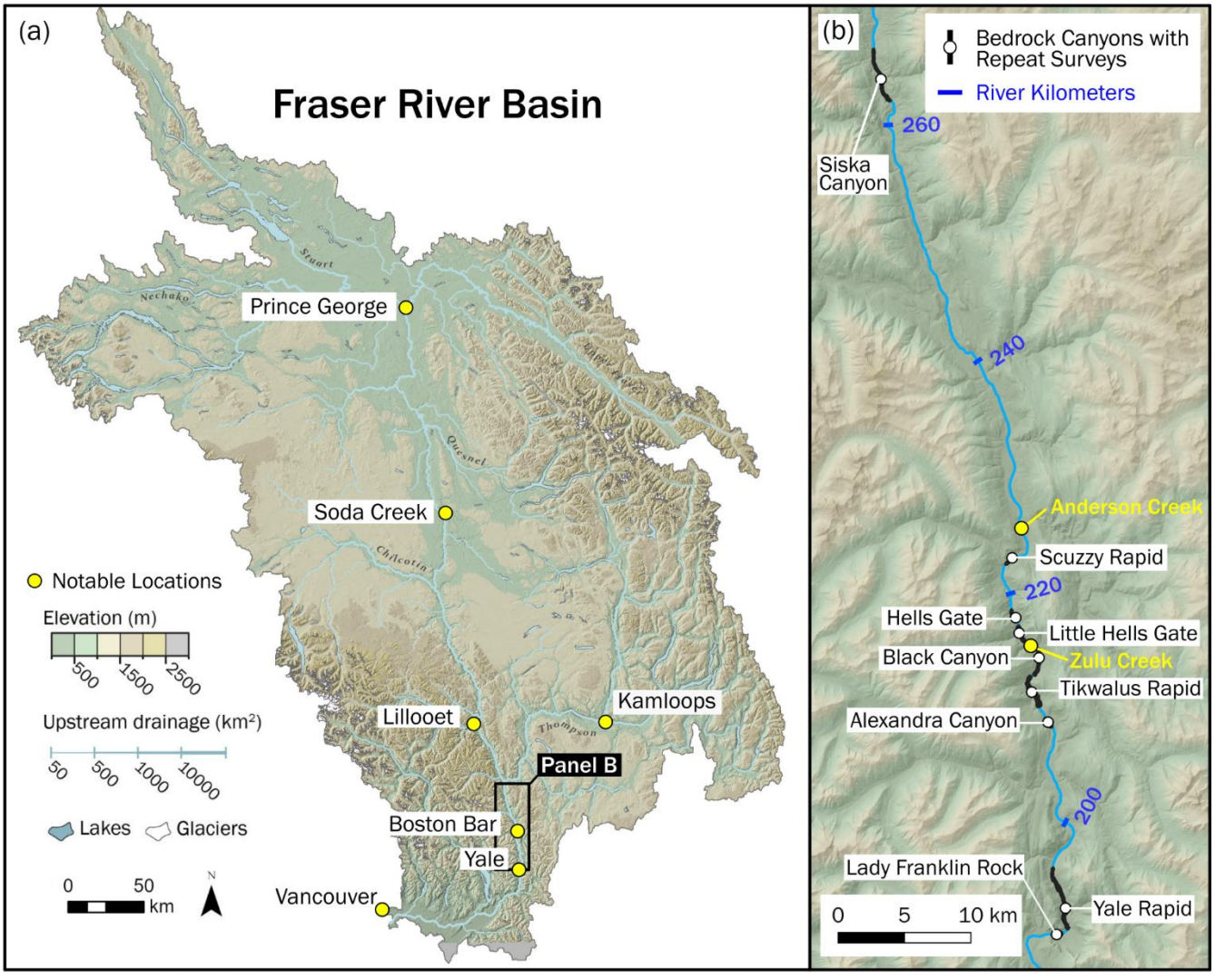


**Figure 2. Fraser River, British Columbia: (a) Fraser River Basin and locations of towns; (b) locations of canyons with repeat surveys as well as Anderson Creek and Zulu Creek tributary confluences.**

https://doi.org/10.5194/egusphere-2026-819
Preprint. Discussion started: 11 March 2026


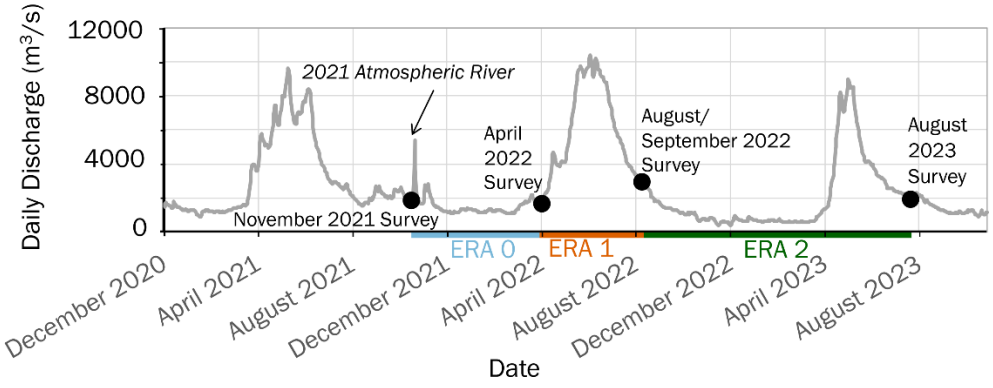


**Figure 3. Hydrograph for the Fraser River at Hope, British Columbia, over a three-year period (December 2020 - December 2023). Data is from the Water Survey of Canada Guage 08MF005. Black circles indicate survey dates. Eras (time elapsed between surveys) are delineated along the x-axis. Era 0 represents the 2021-2022 low-flow season, Era 2 is the 2022 freshet, and Era 2 encompasses the 2022-2023 annual cycle.**

British Columbia experiences atmospheric river precipitation events resulting from extratropical cyclones that contain high amounts of moisture from the Pacific Ocean. Such events cause high rainfall from October to December as atmospheric rivers are orographically lifted when encountering the topography of the region. In November 2021, Southwestern British Columbia experienced an extreme atmospheric river event resulting in flooding and landslides throughout the Fraser Valley and Canyon. The rainfall magnitude was not unusual for Southwestern British Columbia, but the angle of the storm directed it up the Fraser Valley and Canyon affecting infrastructure and transportation corridors (Gillett et al., 2022). Saturated soil from previous storms and rain-on-snow led to an unusual runoff event that caused a series of landslides and debris flows that contributed substantial sediment to the river during an otherwise low flow period (Baird, 2024; Sepúlveda et al., 2023). Our surveys bracket the November 15, 2021, atmospheric river and resulting sediment supply event.

### 2.2 Surveys

Our dataset encompasses nine bedrock canyons with repeat surveys in the Lower Fraser Canyon between Lytton and Yale, British Columbia (Figure 2b). These canyons are representative of the range of width, depth, and velocity observed throughout the Fraser Canyon. Repeat surveys were conducted by boat using a Norbit iWBMS echosounder, operated at 400 kHz, with an integrated Applanix WaveMaster II inertial motion sensor, an AML Minos X sound velocity probe, and inline Trimble GNSS receivers. Range resolution of the Norbit echosounder is < 10 mm. Each survey consists of multiple overlapping passes through major morphological features in which initial centreline passes used a swath angle of 150° - 170° and channel walls were mapped by steering the beams to either side. Data were post-processed in POSPac MMS software using PP-RTX corrections or an RTK base station to improve positioning accuracy. RTX corrections give horizontal and vertical accuracy of < 20 mm and < 50 mm respectively while RTK corrections give horizontal and vertical accuracy of ~8 mm and ~15 mm, respectively. Bathymetric data were manually filtered to remove acoustic noise in QPS Qimera software and point clouds were

https://doi.org/10.5194/egusphere-2026-819
Preprint. Discussion started: 11 March 2026


exported using the NAD83 UTM 10N (Epoch 2002) coordinate system with a CGVD2013 vertical datum. Digital elevation models (DEMs) of bathymetry were generated at a horizontal resolution of 0.5 m. Coverage varies somewhat due to river conditions, but DEMs typically extend bank to bank with coverage to ~1 m below water surface near the banks and lower coverage in places where the river has high velocity, aeration and turbulence levels.

Surveys characterize bed and bank topography of nine individual canyons along the Lower Fraser Canyon (Figure 2b) between 2021 and 2023 (Table 1). All surveys are collected at low to moderate discharges (1500 - 3000 $m^3/s$ at Hope). The first survey was conducted November 10-12, 2021 (discharge at Hope: 1900 – 2050 $m^3/s$) at Yale Rapids and Lady Franklin Rock in advance of the November 15, 2021 atmospheric river and sediment supply event. The second survey took place April 2022 (1560 – 1800 $m^3/s$) in all nine of the canyons before the rising limb of the 2022 freshet. The third survey occurred the same year during the later part of the falling limb in August/September 2022 (1880 – 3330 $m^3/s$) in all nine canyons. The fourth and final survey was conducted August 2023 (1950 – 2110 $m^3/s$) in eight of the canyons (all except Siska Canyon), during the falling limb of the freshet. The elapsed time between surveys is split into three Eras: Era 0 the 2021-2022 low-flow season (November 2021 to April 2022); Era 1 the 2022 freshet (April 2022 to August/September 2022); and Era 2 the 2022-2023 annual cycle (August/September 2022 to August 2023). Era 0 encompasses the 2021-2022 low-flow season showing change in elevation after the atmospheric river precipitation event during winter baseflow, whereas Era 1 characterizes intra-annual change during the following 2022 summer freshet. Era 2 depicts the 2022-2023 annual change cycle, showing changes post-freshet from year to year (Figure 3).

https://doi.org/10.5194/egusphere-2026-819
Preprint. Discussion started: 11 March 2026


**Table 1. Surveys, associated dates, canyons surveyed, and mean daily discharge.**

| Survey | Dates | Canyons Surveyed | Discharge at Hope ($m^3/s$) |
|---|---|---|---|
| November 2021 Survey | November 10, 2021 | Yale Rapids, Lady Franklin Rock | 1990 |
| | November 11, 2021 | Yale Rapids, Lady Franklin Rock | 1900 |
| | November 12, 2021 | Yale Rapids, Lady Franklin Rock | 2050 |
| April 2022 Survey | April 25, 2022 | Siska Canyon | 1560 |
| | April 26, 2022 | Scuzzy Rapid, Hells Gate Canyon, Little Hells Gate Canyon, Black Canyon | 1660 |
| | April 27, 2022 | Tikwalus Rapid, Alexandra Canyon, Yale Rapids, Lady Franklin Rock | 1800 |
| August/September 2022 Survey | August 25, 2022 | Siska Canyon | 3290 |
| | August 26, 2022 | Scuzzy Rapid | 3210 |
| | August 30, 2022 | Yale Rapid, Lady Franklin Rock | 2960 |
| | August 31, 2022 | Yale Rapid, Lady Franklin Rock | 2940 |
| | September 1, 2022 | Yale Rapid, Lady Franklin Rock | 2890 |
| | September 13, 2022 | Tikwalus Rapid, Alexandra Canyon | 2020 |
| | September 14, 2022 | Tikwalus Rapid, Alexandra Canyon, Hells Gate Canyon, Little Hells Gate Canyon, Black Canyon | 1960 |
| | September 15, 2022 | Hells Gate Canyon, Little Hells Gate Canyon, Black Canyon | 1880 |
| August 2023 Survey | August 2, 2023 | Yale Rapids, Lady Franklin Rock | 2110 |
| | August 3, 2023 | Yale Rapids, Lady Franklin Rock | 2060 |
| | August 4, 2023 | Yale Rapids, Lady Franklin Rock | 2020 |
| | August 7, 2023 | Scuzzy Rapid, Hells Gate Canyon | 1950 |
| | August 8, 2023 | Little Hells Gate Canyon, Black Canyon | 1970 |
| | August 9, 2023 | Black Canyon, Tikwalus Rapid | 2020 |
| | August 10, 2023 | Tikwalus Rapid, Alexandra Canyon | 2050 |

*Note: April/May 2022 surveys were corrected using PP-RTX, whereas all other surveys had an RTK base station.*

### 2.3 Morphological categorization

Surveyed canyons were categorized according to the dominant channel morphology as: (1) constriction-pool-widenings (CPWs), (2) rapids, or (3) overfalls, although many of the surveyed canyons have characteristics of multiple bedrock-bound morphologies. CPWs were identified by the presence of a constriction in channel width coinciding with a deep pool, followed by a downstream widening of the channel. Pools can be located within, upstream, or downstream of the constriction (Wright et al., 2022). Due to plunging flows and resulting velocity inversions, the surface velocity is low in these CPWs, meaning there is often no white water visible at the surface in the widenings. Rapids were identified by white water and high velocities at the surface relative to the low surface velocities observed at CPWs, as well as shallower depths relative to CPWs. Overfalls are

https://doi.org/10.5194/egusphere-2026-819
Preprint. Discussion started: 11 March 2026


identified by the presence of a significant drop in water surface elevation without flow detaching from the bed, a hydraulic jump, and visible white water (Venditti, 2026). Our categorization benefits from detailed observations of velocity through the canyons reported in Hurson et al. (in review).

### 2.4 Change detection and analysis

We created a DEM of elevation differences for each Era by subtracting the older of the two surveys from the more recent. Positive changes were then interpreted as sediment deposition, and negative changes as sediment erosion. Given the horizontal and vertical accuracies of our GNSS and echosounder, we elected to ignore changes in topography $\leq 0.1$ m. Difference maps could only be resolved where data was present in both surveys. We use surveys of Tikwalus Rapid to illustrate the workflow in Figure 4, which shows DEMs for the April 2022 survey (DEM A; Figure 4a) and August 2022 survey (DEM B; Figure 4b) which have been processed at the same resolution and are spatially coincident. The differenced DEM shows where the elevation increased due to sediment deposition and decreased due to sediment erosion over the approximately four months of Era 1 which encompasses the 2022 freshet (Figure 4c).

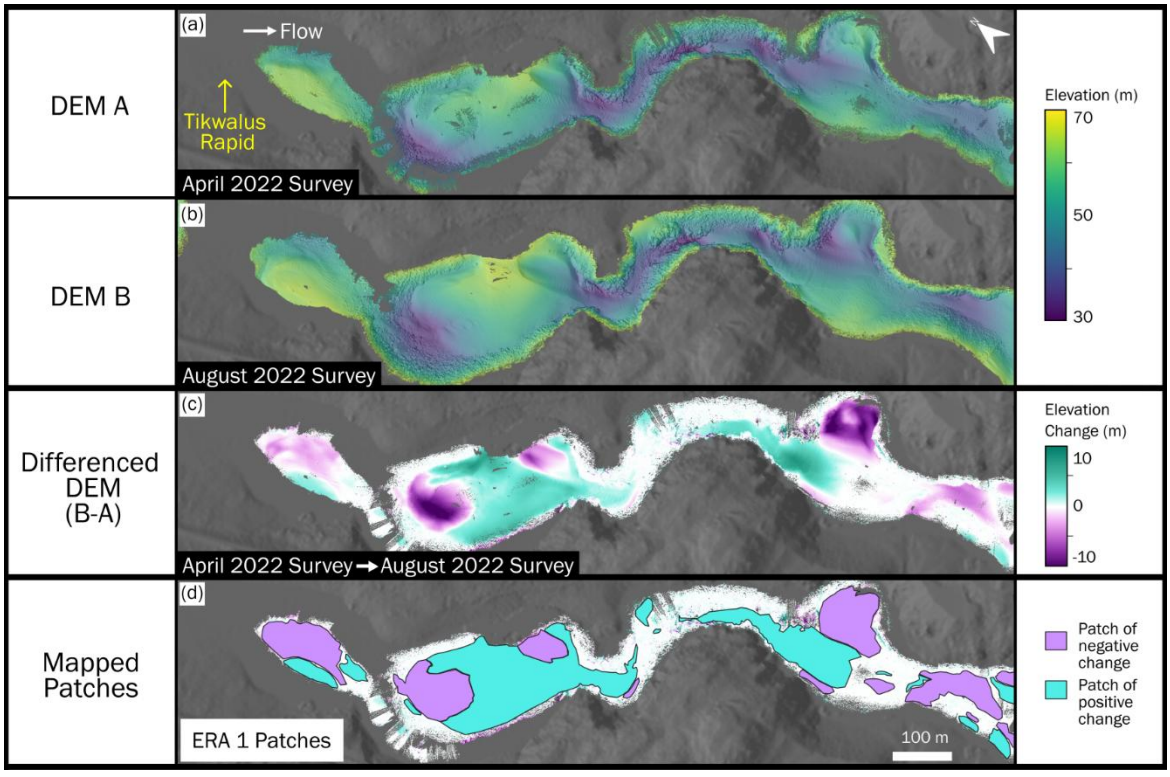


**Figure 4. Visualization of the change detection workflow using repeat surveys at Tikwalus Rapid over Era 1 as an example: (a) bathymetry at Tikwalus Rapids in April 2022; (b) bathymetry at Tikwalus Rapid in August 2022; (c) elevation differences between the two surveys representing change in Era 1 through the 2022 freshet; (d) manually mapped patches of change from Era 1 at Tikwalus Rapid.**

https://doi.org/10.5194/egusphere-2026-819
Preprint. Discussion started: 11 March 2026


The final step in processing DEMs of elevation difference was to delineate distinct patches where we could calculate the change in sediment storage by integrating the elevation difference over each patch area (e.g. Figure 4d). We defined a patch as a spatially contiguous area of deposition or erosion with a zone of near zero change surrounding it. We attempted to automate patch identification, but results failed to show coherent patterns due to many small patches that were difficult to distinguish from survey uncertainty. Therefore, we mapped patches manually, only mapping those patches for which we had high confidence based on factors such as the presence of bedforms, proximity to the banks, consistency of data coverage, knowledge of data collection conditions in the field, and the size of the patch. As a result, mapped patches tended to be larger and closer to the centre of the channel where there is high data density resulting from multiple independent passes of the echosounder. We excluded from the analysis smaller potential patches located in regions with low data coverage, typically close to the banks, due to low confidence in the accuracy of patch boundaries. The volume of change in each patch was measured as the sum of the change in each pixel multiplied by pixel area (0.25 $m^2$). Additionally, the patch area and location along the Fraser River centreline were extracted. The smallest patch size considered was 2 $m^2$.

We calculated the dynamic sediment storage volume through surveyed reaches as the difference between survey bathymetry and the minimum elevation observed throughout all the surveys. This method was developed to establish the contribution of alluvial sediment cover in each bathymetric survey, as well as to reveal spatial and temporal changes in cover. We created a minimum elevation DEM in which each pixel represents the lowest observed bed elevation in that area over all the surveys. We then created DEMs of difference by subtracting the minimum elevation DEM from each survey bathymetry DEM. This elevation change was then multiplied by pixel area (0.25 $m^2$) to yield the volume of alluvial bed storage. The calculation of dynamic storage was restricted to regions within mapped patches of detectable change as these excluded areas with low survey confidence that may introduce error. Alluvial storage identified within these areas is used as a metric for volume of dynamic sediment storage at each location for each survey. The dynamic storage volume was calculated at the same 0.5 m resolution as the DEMs, and values were grouped by the closest river meter location along the Fraser River centreline. The grouped points were then summed to reveal total dynamic storage volume along each 20 m section of the channel.

## 3 Results

### 3.1 Morphology of canyons

We classify four canyons as having CPW morphology: Siska Canyon, Black Canyon, Alexandra Canyon, and Lady Franklin Rock (Figure 5a, b, c, d). Each of these reaches has a deep pool either upstream, within, or downstream of the constriction. This deep pool extends downstream into the beginning of the widening before ultimately shallowing within this wide section. The deep slot-like features observed in constrictions of Siska Canyon, Alexandra Canyon, and Lady Franklin Rock resemble those found in flume experiments of CPW bed topography (Kusack et al., 2024). Lady Franklin Rock has a mixed morphology

https://doi.org/10.5194/egusphere-2026-819
Preprint. Discussion started: 11 March 2026


with characteristics of both CPWs and rapids due to the slot through the constriction forming lateral ledges resulting in shallow flow and white water at the surface.

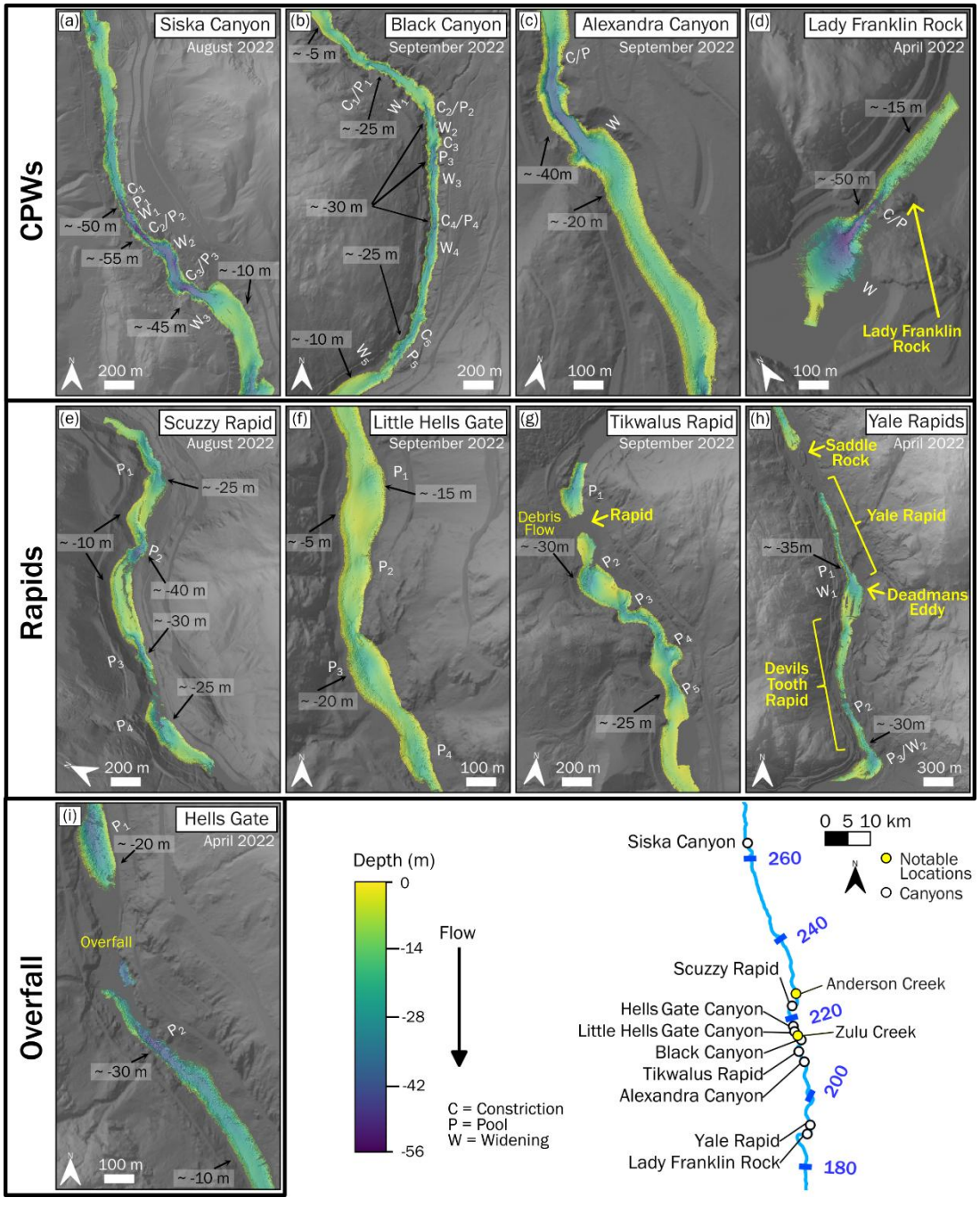


**Figure 5. Canyon bathymetry as depth below water surface at sites with repeat surveys. Reaches are categorized based on morphodynamic type. Approximate depth values are labelled at select locations with notable features. Prominent morphologic features are labelled as well. Streamwise positions are mapped. See supplement for bathymetric maps of all surveys.**

https://doi.org/10.5194/egusphere-2026-819
Preprint. Discussion started: 11 March 2026


We identified four canyons dominated by rapids, characterized by shallow flow and white water, including: Scuzzy Rapid, Little Hells Gate Canyon, Tikwalus Rapid, and the multiple rapids within Yale Rapids (Figure 5e, f, g, h). The rapids have variation in both the width and bed morphology, with narrow slot pools and ledges along the banks. Little Hells Gate Canyon and Tikwalus Rapid are typical rapids while Yale Rapids and Scuzzy Rapid have a somewhat more diverse morphology. Little Hells Gate Canyon has shallow flow and whitewater at the surface along its whole length and less distinct pools (Figure 5f). Tikwalus Rapid is formed by a debris fan (Venditti, 2026) delivered by a debris flow during the November 2021 atmospheric river (Baird, 2024). The channel is partially constricted by the debris fan resulting in a standing wave train and white water at the surface (Figure 5g). Prior to the 2021 debris flow, the canyon where Tikwalus Rapid formed had CPW morphology. Scuzzy Rapid has bedrock-step rapid morphology (Venditti, 2026) but also has characteristics of CPWs. There are constrictions with deep pools, but also sections of shallow flow that produce white water conditions (Figure 5e). Yale Rapids is a series of bedrock-step rapids that have characteristics of CPWs (Venditti, 2026). The reach referred to as Yale Rapids includes a rapid at Saddle Rock where the channel splits around a bedrock island, the eponymous Yale Rapid that has a narrow slot pool cut down the channel centreline and shallow flow over ledges on either side of the channel, a widening called Deadmans Eddy, and another rapid called Devils Tooth Rapid that also has a narrow slot and shelves (Figure 5h).

Hells Gate Canyon has a constricted overfall morphology (Venditti, 2026). Upstream of the overfall the flow is shallow, then accelerates through a constriction, followed by a ~2.5 m vertical drop in water surface elevation that produces a hydraulic jump, and a 30 m deep scour pool downstream (Figure 5i). Hells Gate Canyon had a CPW morphology until 1912 when blasting associated with railway construction resulted in debris deposition into the constriction creating a boulder-step overfall, which was later exacerbated by a rockfall in 1914 (Evenden, 2004). Subsequent blasting has deepened the channel creating a constricted overfall morphology. Our bathymetry is not well resolved through Hells Gate Canyon at the overfall because the flow is too aerated for multibeam observations, but we have observations upstream and downstream of the overfall that reveal sedimentation patterns.

### 3.2 Spatial changes in sediment storage

Sediment storage varies through the canyons and Eras as evidenced by mapped patches of erosion and deposition (Table 2, Figure 6). All canyons, excluding Hells Gate Canyon (the overfall), have patches that aggrade and patches that erode within each Era. Elevation changes as high as 15 m are observed. Yet, the mean elevation change for each patch has a median of just ~0.7 m for all patches. The median patch area is ~990 $m^2$, and patch area is log-normally distributed. The smallest patch observed was ~12 $m^2$ and the largest was ~85,900 $m^2$. We observe patch volumes, which are also log-normally distributed, ranging from ~4 $m^3$ to ~325,700 $m^3$. The median patch volume for all canyons over all Eras, independent of direction of change, is ~640 $m^3$. When we test for differences between the morphodynamic type assigned to the canyon they are found in, or the Era they are observed in, we do not find any statistically significant differences in absolute mean elevation change, area,

https://doi.org/10.5194/egusphere-2026-819
Preprint. Discussion started: 11 March 2026


or absolute volume of patches. However, the overfall has by far the lowest percentage patch area to survey area compared to the other morphologies.

**Table 2. Median and inter-quartile range (IQR) for absolute mean vertical change, patch area, and absolute volume of patches. Statistics are calculated for all patches as well as subgroupings based on direction of change, morphodynamic type, and Era. Results are rounded to the nearest unit for area and absolute volume, and to the nearest hundredth of a meter for absolute mean elevation change.**

| Group | N | Abs of Mean Vertical Change (m) | | Area ($m^2$) | | Abs Volume ($m^3$) | |
|---|---|---|---|---|---|---|---|
| | | Median | IQR | Median | IQR | Median | IQR |
| All Patches | 390 | 0.69 | 0.97 | 993 | 3172 | 642 | 3387 |
| Erosion | 190 | 0.79 | 1.01 | 1103 | 4034 | 735 | 4725 |
| Deposition | 200 | 0.65 | 0.87 | 827 | 2461 | 519 | 2697 |
| CPWs | 129 | 0.66 | 1.01 | 856 | 2772 | 515 | 2426 |
| Overfall | 5 | 0.99 | 1.13 | 2970 | 3032 | 1739 | 1251 |
| Rapids | 256 | 0.70 | 0.94 | 1034 | 3128 | 669 | 3723 |
| Era 0 | 27 | 0.43 | 0.65 | 913 | 1974 | 613 | 610 |
| Era 1 | 197 | 0.68 | 1.05 | 879 | 2440 | 575 | 2392 |
| Era 2 | 166 | 0.77 | 0.84 | 1164 | 4458 | 765 | 4936 |

https://doi.org/10.5194/egusphere-2026-819
Preprint. Discussion started: 11 March 2026


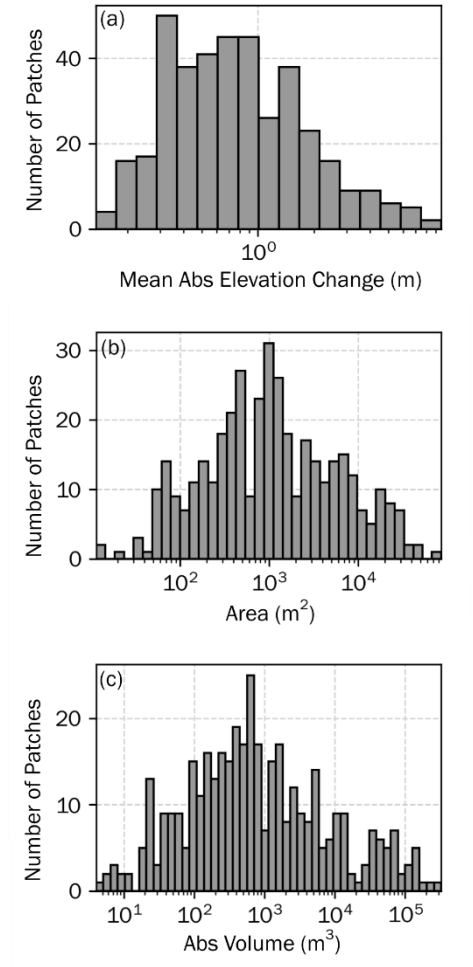


**Figure 6. Distribution of mapped patches from all Eras, morphodynamic types, and directions of change based on patch (a) mean absolute elevation change (b) area, and (c) absolute volume. See Table 2 for measured statistics.**

CPWs tend to have channel-spanning patches, while rapids have more spatial variation in patches throughout the reach, and the overfall had no obvious erosion or deposition in the pool downstream of the vertical elevation drop (Figure 7). Throughout all the Eras, CPWs tended to have large continuous patches, extending downstream at length scales longer than the channel width, located throughout the pool and constriction. These channel-spanning patches also tend to follow the morphology of the inner slots through constrictions (Figure 7a, b, c, d). Discerning a pattern of change within the rapid morphology is challenging due to higher variation in relative patch locations and magnitudes. However, there appears to be a more prominent alternation between erosion and depositional changes in storage in subsequent downstream patches, as well as across the channel width (Figure 7e, f, g, h). Our surveyed overfall, Hells Gate Canyon (Figure 7i), has negligible elevation change downstream of the overfall (< 1 m vertical change).

https://doi.org/10.5194/egusphere-2026-819
Preprint. Discussion started: 11 March 2026


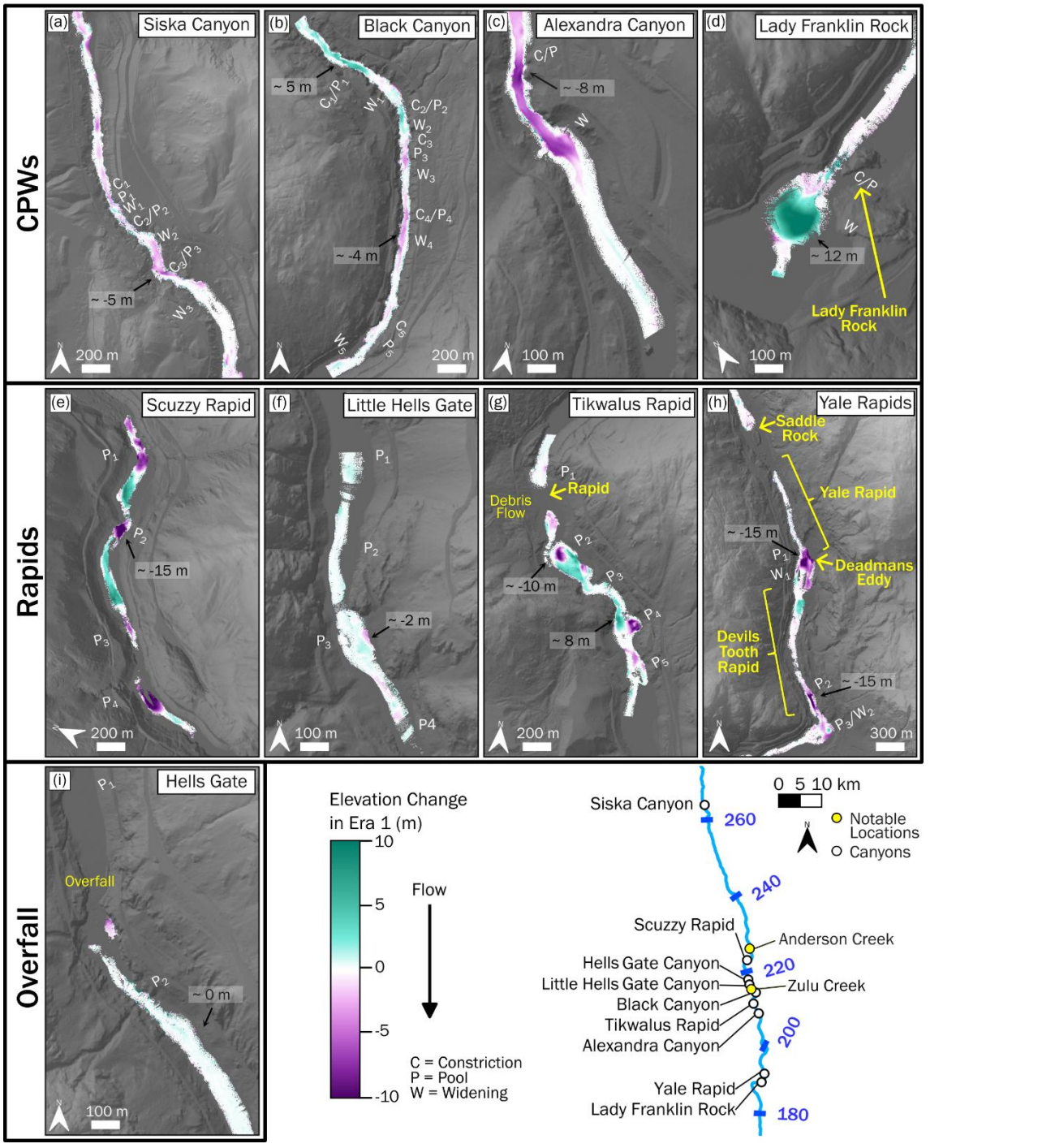


**Figure 7. Change in elevation during Era 1 at all sites, with regions of deposition represented by positive change, and erosion by negative change. Approximate elevation change values are labelled at select locations with notable features. Prominent morphologic features labelled in Figure 5 are also visible. Streamwise positions are mapped. See supplement for maps of change in bathymetry over all the Eras.**

https://doi.org/10.5194/egusphere-2026-819
Preprint. Discussion started: 11 March 2026


While the volume of dynamic storage changes between different morphologies and Eras, the locations of storage are consistent over time (Figure 8). Peaks in dynamic storage occur at locations where there are large channel-spanning patches associated with CPWs as well as throughout rapid reaches. However, the volume of dynamic storage varies at these locations. For instance, at Yale Rapids and Lady Franklin Rock there is significant fluctuation in the magnitude of dynamic storage peaks, with increases and decreases in storage varying from peak to peak and survey to survey. In November 2021 the three dominant locations with peaks in storage (located between river kilometres 189 and 193) have volumes between ~6000 $m^3$ and ~12,000 $m^3$. In April 2022 these same locations have storage in the range of ~12,000 $m^3$ to ~20,000 $m^3$. In August 2022, the two upstream locations have decreased to a dynamic storage around ~6000 $m^3$ while the most downstream location increases dramatically to ~44,000 $m^3$. Finally, in August 2023 the peaks range from ~6000 $m^3$ to ~22,000 $m^3$. Despite substantial changes in the magnitude of dynamic storage in each of the surveys, the location of the peaks in storage remains consistent. The most upstream location has the greatest dynamic storage in April 2022 and August 2023, while the middle location is the greatest in November 2021, and the most downstream location has the highest dynamic storage observed in all the surveys and canyons in August 2022.

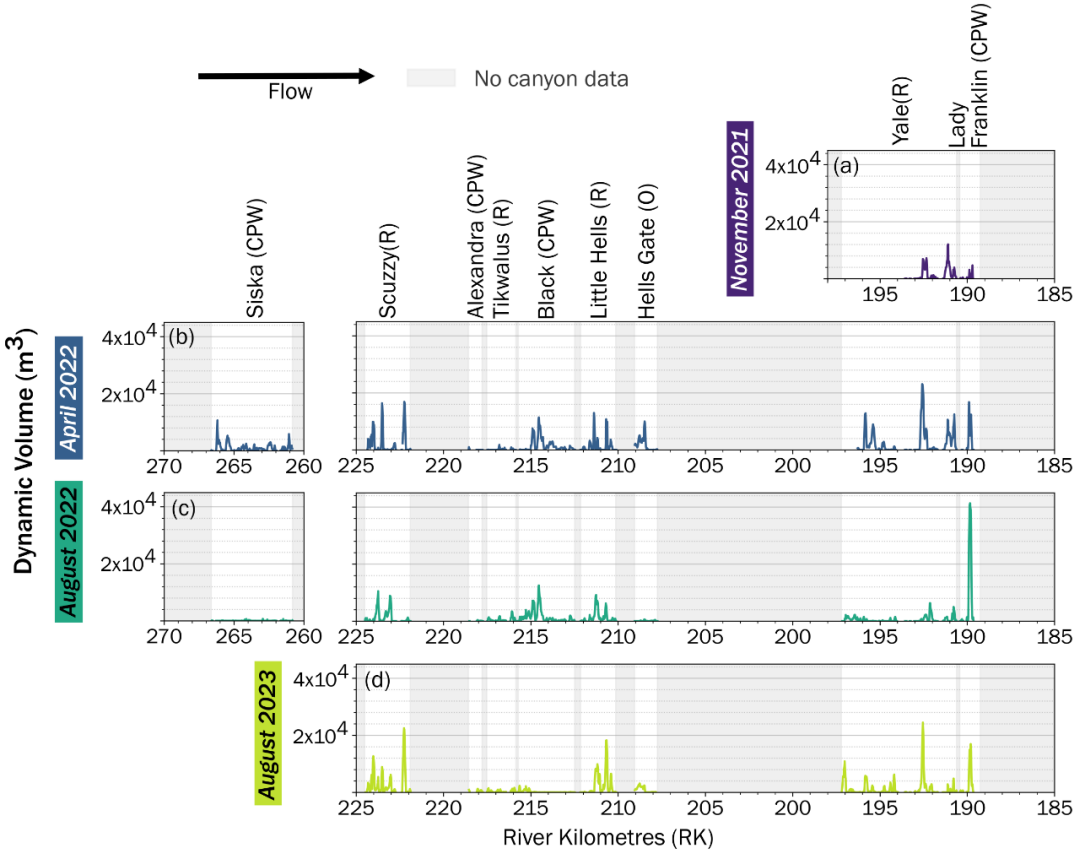


**Figure 8. Dynamic sediment storage volume, calculated as difference from minimum elevation observed over all surveys for each canyon and Era surveyed. Canyon survey locations are plotted along river kilometers. Volume is summed over 20 m longitudinal increments. In brackets after canyon names their morphology is noted ("CPW" for constriction-pool-widenings, "R" for rapids, and "O" for the overfall).**

https://doi.org/10.5194/egusphere-2026-819
Preprint. Discussion started: 11 March 2026


Patch dynamics within Black Canyon, Tikwalus Rapid, and Alexandra Canyon include cases where patches merged, split, or changed direction over different Eras; these adjustments varied over the same flow period even within the same canyon morphology (Figure 9). At Black Canyon, the most upstream patch shifted from deposition in Era 1 during the 2022 freshet ($B_1$; Figure 9a) to erosion in Era 2 through the 2022-2023 annual cycle ($B'_1$; Figure 9b). We observe that patches merged at Black Canyon, with one depositional ($B_2$; Figure 9a) and two erosional patches ($B_3$ and $B_4$, Figure 9a) in Era 1 becoming a single erosional patch ($B'_{234}$, Figure 9b) in Era 2. At Tikwalus Rapid, the upstream erosional patch in Era 1 ($T_1$; Figure 9c) split into multiple patches of both erosion and deposition in Era 2 ($T'_1$; Figure 8d), while the two downstream patches, one depositional ($T_2$; Figure 9c) and the other erosional ($T_3$; Figure 9c) in Era 1, combined into a single depositional patch in Era 2 ($T'_{23}$; Figure 9d). At Alexandra Canyon, the large dominant patch ($A_1$; Figure 9e, $A'_1$; Figure 9f) that extends through the constriction and into the widening, remained in the same location between Eras, yet switched from erosional in Era 1 to depositional in Era 2. Importantly, even as these patches merged, split, and changed direction, the planform area (i.e. footprint) of sediment storage change overall remains almost entirely consistent over time.

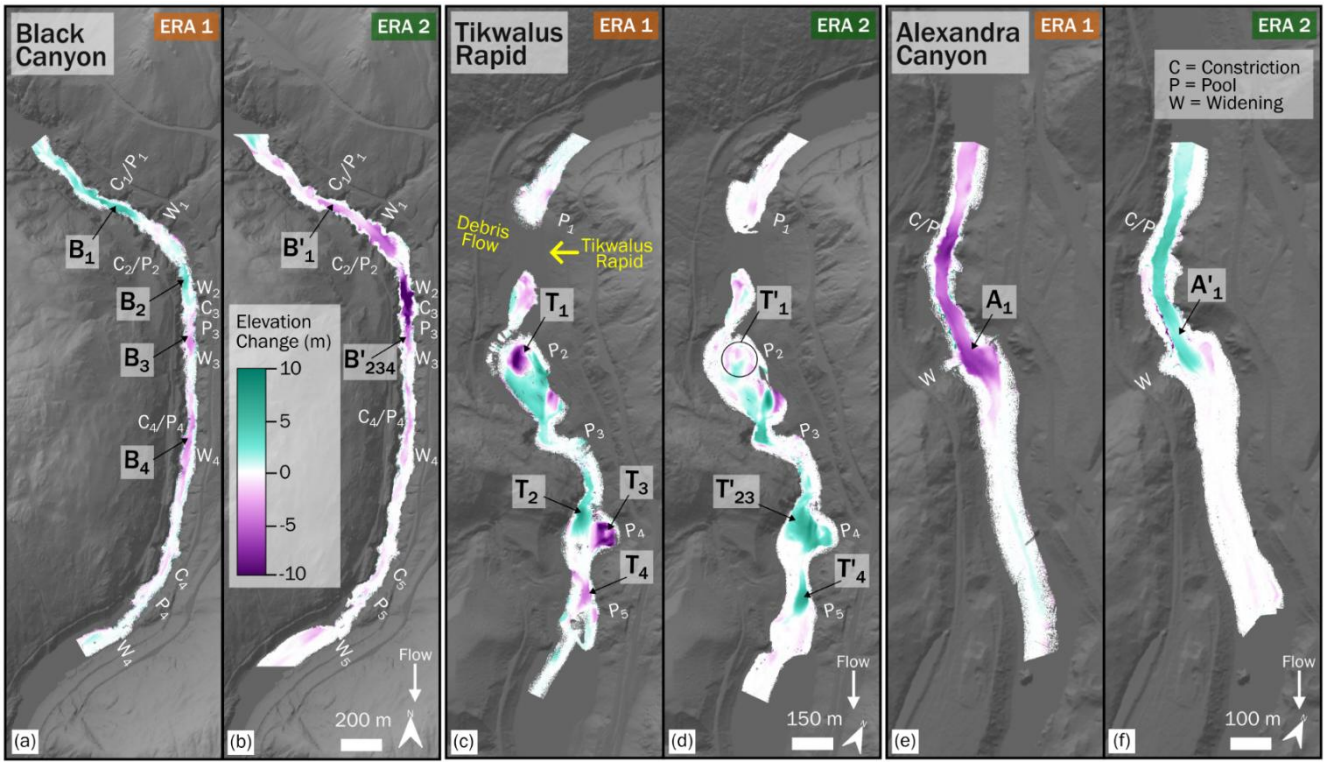


**Figure 9. Elevation changes at Black Canyon, Tikwalus Rapid, and Alexandra Canyon for Era 1 and Era 2. Prominent morphological features are labeled. Patches discussed in text are labeled with the first letter of the canyon name, and a numbered subscript for identification, while prime notation is used to distinguish between Eras.**

https://doi.org/10.5194/egusphere-2026-819
Preprint. Discussion started: 11 March 2026


### 3.3 Sediment staging through the canyons

We refer to the short-term process of localized sediment collection, storage, and release as sediment 'staging.' The complex patch behaviour observed (e.g. merging, splitting, changing between erosion and deposition) is evidence of sediment staging through the canyons following the major sediment supply event in 2021. Black Canyon, Tikwalus Rapid, and Alexandra Canyon, occur in a downstream sequence with short intervening sections that are not bedrock-bound. Upstream of Black Canyon is the Zulu Creek debris fan and the Anderson Creek confluence delta which grew substantially following the 2021 atmospheric river. A debris fan is also located between Black Canyon and Alexandra Canyon that formed Tikwalus Rapid after the November 2021 supply event. Topographic differencing indicates that the upstream end of Black Canyon and the downstream end of Tikwalus rapid aggraded in Era 1 through the 2022 freshet suggesting that a large pulse of sediment was added to the channel following the 2021 supply event (Figure 9). In Era 2 through the 2022-2023 annual cycle, the Black Canyon deposit eroded and the sediment deposit downstream of Tikwalus Rapid passed further downstream. Alexandra Canyon eroded in Era 1, then aggraded in Era 2, having received sediment from Black Canyon and Tikwalus Rapid. This suggests sediment is passed from canyon to canyon and that the direction of change in sediment storage reflects sediment supply events.

There is also evidence that sediment staging occurred at Yale Rapids and Lady Franklin Rock Canyons in response to a high sediment input event (Figure 10). Change in sediment storage primarily occurred along this reach in three wide sections of the channel: downstream of Yale Rapid in Deadmans Eddy ($W_1$; Figure 10), just downstream of Devils Tooth Rapid ($W_2$; Figure 10), and downstream of Lady Franklin Rock ($W_3$; Figure 10). Surveys of these reaches at low flow, before and following the November 2021 supply event (Era 0), reveal deposition in all three wide sections of the channel ($Y_1$, $Y_2$, and $L_1$; Figure 10a). During the subsequent high flow period (Era 1) Deadmans Eddy ($Y'_1$; Figure 10b) as well as at the wide section downstream of Devils Tooth Rapid ($Y'_2$; Figure 10b) show a shift to erosion, however, the widening at Lady Franklin Rock continues to aggrade, having received the sediment from the upstream widenings ($L'_1$; Figure 10b). Over the following low and high flow season (Era 2), Deadmans Eddy ($Y''_1$; Figure 10c) began to aggrade again, yet the wide section downstream of Devils Tooth Rapid ($Y''_2$; Figure 10c) continued to erode, while substantial sediment erosion occurred downstream of Lady Franklin Rock ($L''_1$; Figure 10c). The November 2021 atmospheric river delivered a large volume of sediment to the Fraser Canyon, but that sediment was primarily delivered to specific points along the channel through tributaries or mass movement events. As temporal proximity to the event increases, sediment appears to have been staged through the Yale Rapids to Lady Franklin Rock Canyons reach as topographic changes occurred in a propagating erosive pattern downstream.

https://doi.org/10.5194/egusphere-2026-819
Preprint. Discussion started: 11 March 2026


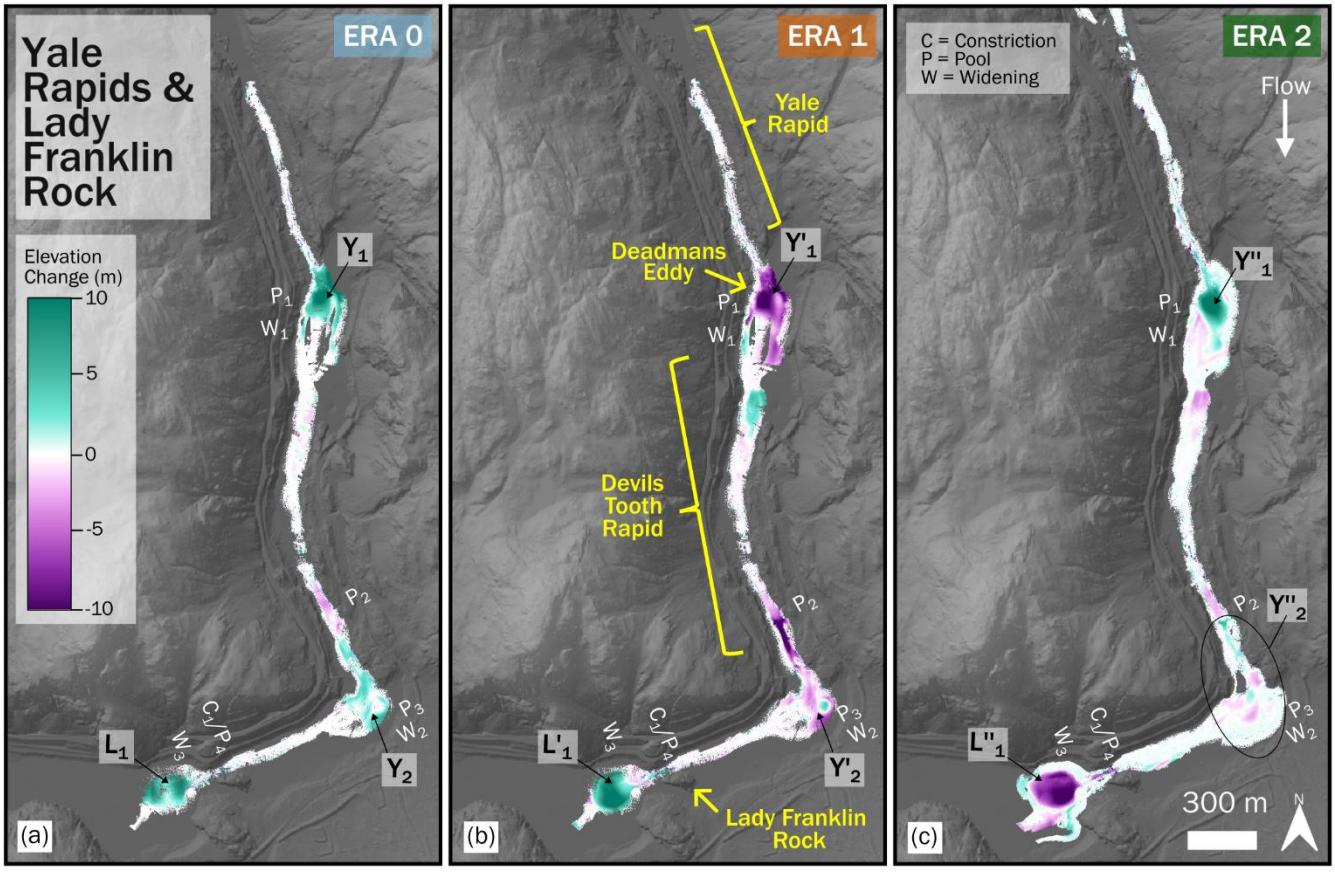


**Figure 10. Elevation changes at Yale Rapids and Lady Franklin Rock for Era 0, Era 1 and Era 2. Prominent morphological features are labeled. Patches discussed in text are labeled with the first letter of the canyon name, and a numbered subscript for identification, while prime notation is used to distinguish between Eras.**

The calculated flux divergence of volume change throughout the canyons shows that there is a reversal in dominant sediment storage signals between Era 0 the 2021-2022 low-flow season (depositional), Era 1 the 2022 freshet (erosive), and Era 2 the 2022-2023 annual cycle (depositional) (Figure 11). Flux divergence is calculated as cumulative change in patch volume summed from upstream to downstream through all surveyed canyons. Era 0 has the lowest data coverage (only spanning Yale Rapids to Lady Franklin Rock) but even so we measured a net accumulation of ~509,000 $m^3$ over the approximately five-month period between surveys. Era 1 has the highest coverage (all nine canyons) and a net erosion of approximately – 764,000 $m^3$ over the four-month period between surveys. Era 2 has coverage in all canyons except Siska Canyon and a net depositional flux divergence of ~148,000 $m^3$ over the year between surveys. The locations of the greatest changes in flux divergence occur in the same reaches between the Eras, such as river kilometre ~193 in Yale Rapids or ~190 in Lady Franklin Rock. Notably, sediment storage change is dramatic at pools within CPW morphologies (e.g. Black and Alexandra Canyons in Figure 9), as well as widenings downstream of canyons and rapids (e.g. Tikwalus Rapid in Figure 9; Figure 10).

https://doi.org/10.5194/egusphere-2026-819
Preprint. Discussion started: 11 March 2026


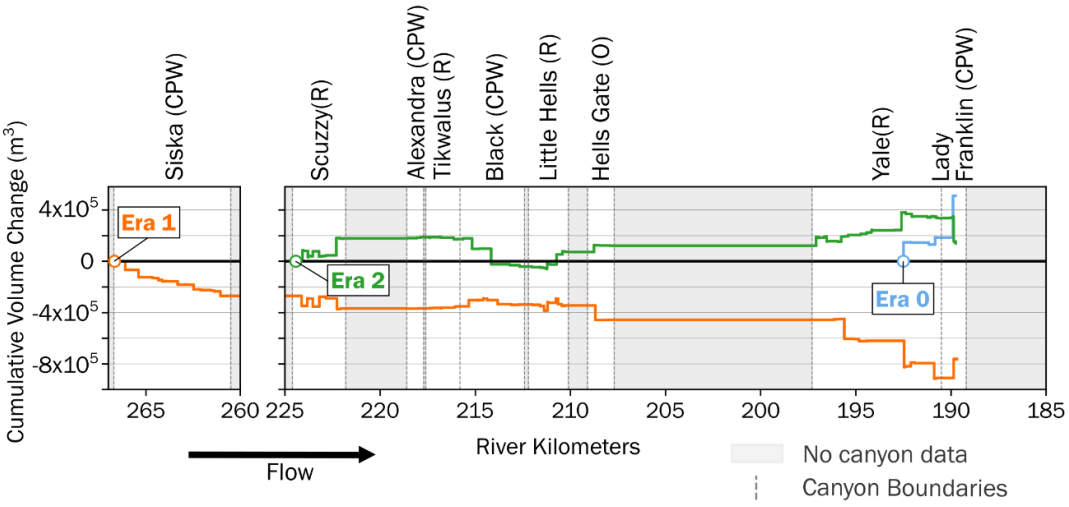


**Figure 11. Flux divergence through the surveyed canyons for each Era, calculated as cumulative change in patch volume summed from upstream to downstream. Analysis shows that Era 0 and Era 2 were dominated by deposition while erosion dominated during Era 1. The upstream-most point with data is labeled for each Era. Regions without survey data are shaded grey, so flux divergence is assumed to be constant throughout these reaches. In brackets after canyon names their morphology is noted ("CPW" for constriction-pool-widenings, "R" for rapids, and "O" for the overfall).**

### 3.4 Comparing the roles of morphology and staging in sediment storage

To compare the influence of morphology versus sediment staging on sediment movement through the canyons, we explored changes in patch area and volume. We found that total patch footprint was relatively consistent while net volume change was much more dynamic between surveys, indicating that changes in storage need not correspond with changes in patch area (Figure 12). Total mapped patch area between Era 1 the 2022 freshet and Era 2 the 2022-2023 annual cycle was similar for each canyon, indicating a relatively consistent patch footprint over both timesteps (Figure 12a). The only exception is Yale Rapids which had a greater patch area in Era 2 due to a substantial increase in surveyed area. The direction of change in volume can be assessed by plotting Era 1 and 2 volume changes across four quadrants (Figure 12b). If there was no pattern in volume change between the Eras, then we would expect to see points in every quadrant. Quadrants II and IV indicate the same direction of net change between Eras and Quadrants I and III indicate opposite change. Individual patch volume within each canyon had wide variation, but net volume changes are inversely related between Era 1 and 2 (Figure 12b). In general, the canyons that had net erosion in one Era had net deposition in the next Era, or vice versa. This was true for all sites, although Hells Gate Canyon and Little Hells Gate Canyon had very low net values in both Eras. Both rapids and CPWs had large net volumes changes (>10,000 $m^3$) in at least one of the Eras, though the magnitude depends on the individual canyon. The range of net volume change in Era 1 during the 2022 freshet was greater than Era 2 through the 2022-2023 annual cycle, meaning the net volume change was not completely recovered between surveys. Our results indicate patch footprint does not change substantially, but net volume changes occur because the thickness of alluvial deposits change. Additionally, the percentage of the total survey area in which patches occur is independent of the magnitude of net volume change (Figure 12c). There was

https://doi.org/10.5194/egusphere-2026-819
Preprint. Discussion started: 11 March 2026


substantial variation in the fraction of survey area where storage change occurs, ranging from 9% to 68%, yet these changes do not appear to depend on the resulting net volume change throughout the canyon reach. We therefore observe substantial changes in sediment storage without substantial changes in patch footprint.

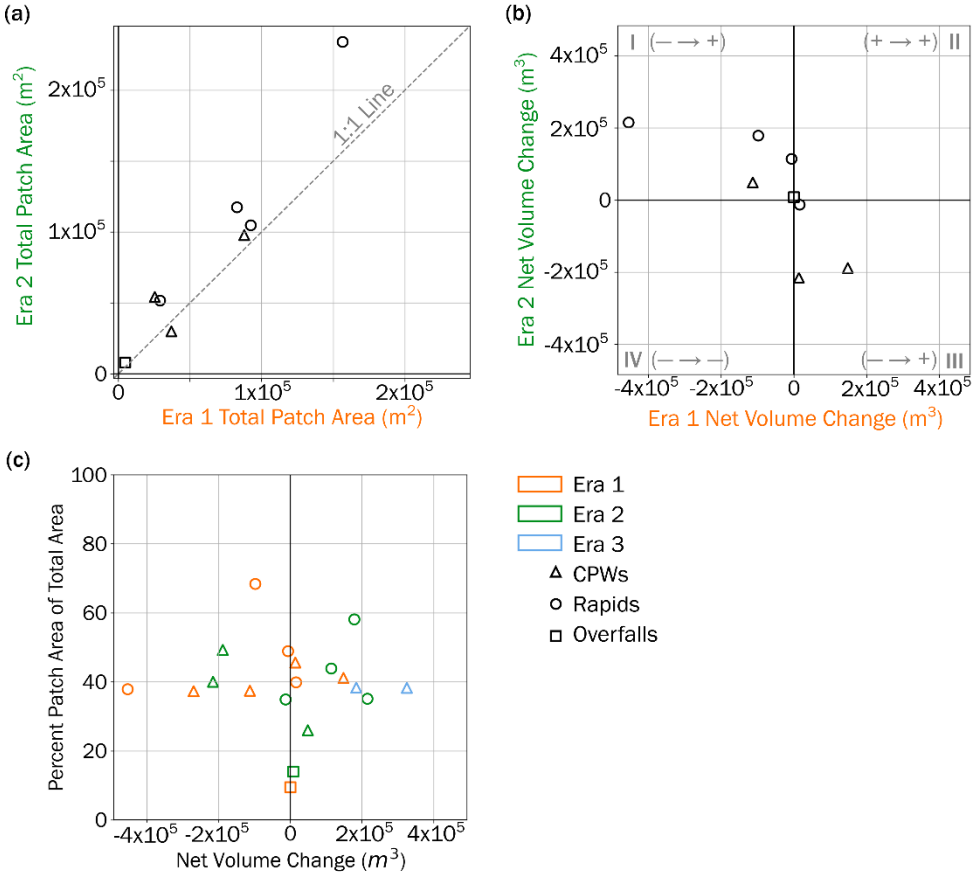


**Figure 12. (a) Comparison of total patch area mapped within each canyon over Era 1 and 2. All canyons with surveys bracketing both Eras were plotted (Siska Canyon therefore excluded). The dashed line indicates 1:1. (b) Comparison of net volume change within each canyon over Era 1 and 2 (again, Siska Canyon therefore excluded). Quadrants I and III indicate a shift between deposition and erosion for canyons depending on the Era. Quadrants II and IV indicate a consistent direction of change over both Eras. (c) Plot of the percentage of patch area of the total survey area against the net volume change observed for each canyon in each Era.**

## 4 Discussion

### 4.1 Morphological controls on sediment storage

Spatial patterns in elevation change appear to align with understanding of end member morphodynamic types outlined by Venditti (2026). CPWs have channel-spanning continuous patches of either erosion or deposition, extending from upstream of the constriction with a slot-like shape, through the pool and into the widening (Figure 13a, d). Therefore, it appears that the

https://doi.org/10.5194/egusphere-2026-819
Preprint. Discussion started: 11 March 2026


deep pools associated with CPWs are locations of sediment storage. Rapids exhibit alternation between patches of erosion and deposition throughout the reach length and channel width (Figure 13b, e). Flow in rapids is chaotic and relatively shallow, leading to the most complex patch behaviour being observed in these reaches. The overfall has negligible storage change throughout its reach (Figure 13c, f). This is likely because upstream of the overfall flow is fast and shallow, while downstream the impinging jet prevents deposition. Additionally, throughout all sites, areas without patches are more common along the margins of the channel suggesting sediment transport also tends to favor the center of the river; however, data analysis also favoured the centre of the channel due to survey coverage and uncertainty. While the location of storage appears in a pattern related to morphology, whether sediment is deposited or eroded in these locations does not.

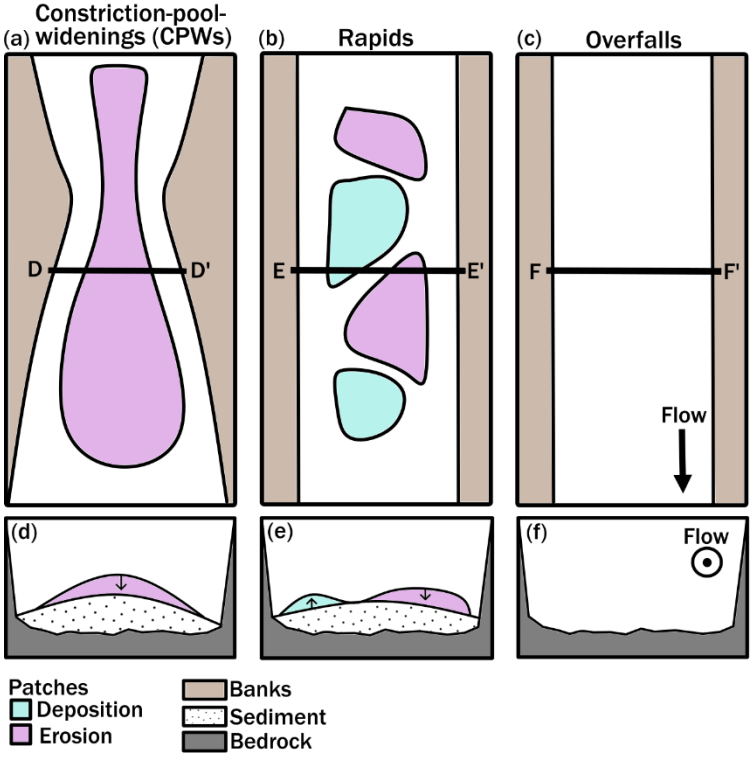


**Figure 13. Cartoon of general patterns of elevation change observed at each morphology. Planform view of patch patterns for (a) CPWs, (b) rapids, and (c) overfalls is simplified based on observations for comparison of general patterns. Additionally, simplified cross sectional views of patch dynamics are shown in (d) for typical CPW morphology (although change may be erosional or depositional), (e) for potential rapid morphology, and (f) for likely overfall morphology based on observations.**

There is a wide range of potential storage volumes associated with a given alluvial bed cover fraction. We observe elevation changes between surveys to be predominantly from alluvial-to-alluvial cover, and do not see evidence of significant changes in bedrock exposure (i.e. alluvial cover encroachment). An example of this can be seen at Tikwalus Rapid (Figure 4a, b), where the bed texture indicates consistent alluvial cover between surveys (through visual distinctions between roughness and the presence of bedforms) except for some very small areas where bedrock exposure may change near the banks as the thickness

https://doi.org/10.5194/egusphere-2026-819
Preprint. Discussion started: 11 March 2026


of deposits fluctuate. This has implications on our understanding of how sediment storage in bedrock channels is scaled with the degree of alluvial bed cover, as our findings indicate that substantial storage changes can occur without a change in the bedrock exposure. In bedrock channels we expect that overall changes in storage will average to zero, however, our results indicate that a dynamic equilibrium exists with fluctuations around a mean sediment cover due to the localized storage capacity of complex bedrock channel morphologies.

It is important to recognize that our surveys are all from low flow conditions. Observation from Hurson et al. (2022) suggest that at moderate flows, the sediment cover is eroded to bedrock. Our annual surveys suggest that there are fluctuations about a mean sediment cover at low flows, and that the bed is not fully exposed. The mean cover is dependent on hillslope-derived sediment supply from upstream and the staging of sediment through canyons. At moderate to high flows, the bed can be exposed, which limits the period when vertical erosion can occur in a canyon.

### 4.2 Storage response to sediment supply events

Reaches with the same morphologies often behave similarly, but observed differences suggest that transient sediment-supply generates an overlapping signal that modifies the underlying influence of channel morphology on sediment dynamics. It is therefore unlikely morphology is the sole influence on sediment storage. Decoupling the impact of morphology and sediment supply on sediment storage is difficult because channels are locally responding to both pulses of sediment moving downstream as well as local flow conditions and morphology. This has been observed in other landscapes where patterns of temporary sediment storage are dependent on channel morphology and staging, influencing the rate at which a pulse of sediment propagates through a system as well as its residence time in different channel locations (e.g. Cook et al., 2020; Gran and Czuba, 2017; Kuo and Brierley, 2014). In a purely morphologically controlled system with a consistent hydrograph pattern and constant sediment supply, we would expect sediment to deposit and erode in patterns dependant on canyon morphology, with high and low flows exacting predictable and repetitive changes locally. This aligns with findings by Hurson et al. (2022) that there is intra-annual variation in the sediment storage in Alexandra Canyon with thick alluvial deposits forming at low flow and being eroded at high flow. In contrast, with a purely sediment supply controlled system, we would expect sediment to move through as a pulse originating from its input location and propagating downstream during high flows, resulting in varied responses between high and low flows locally. Our observed sediment storage patterns reveal overlapping effects of morphology and sediment supply variation.

The capacity for reaches to serve as sediment staging zones is due to their proximity to upstream inputs, the timing of inputs in relation to flow magnitude, and their morphological features. The signals observed at Yale Rapids and Lady Franklin Rock show the potential for some reaches to control the rate of downstream sediment movement, and the influence of their bed cover change on subsequent change dynamics downstream. For instance, wide sections such as Deadmans Eddy at Yale Rapids appear to act as storage zones for incoming sediment. Subsequent clearing of stored sediment in these potential storage zones

https://doi.org/10.5194/egusphere-2026-819
Preprint. Discussion started: 11 March 2026


appears to have impacted storage downstream of these locations. An explanation for the variation in the dominance of erosion versus deposition in these wide sections is to view their signals in relation to their relative streamwise positions. In Era 0 after the atmospheric river, all three wide sections (Deadmans Eddy, just downstream of Devils Tooth Rapid, and at Lady Franklin Rock) experience deposition, likely due to the influx of sediment into the channel sourced from the hillslopes. In Era 1, the following freshet causes the two upstream sections (Deadmans Eddy and just downstream of Devils Tooth Rapid) to shift to erosion, while the downstream section at Lady Franklin Rock continues to be a location of deposition. The sediment eroded from the upstream wide sections provides continued sediment input and deposition to the downstream section. Across the entire next year in Era 2, the upstream sections begin to aggrade again, ceasing the downstream movement of this sediment to the final widening, which may relate to the observed erosion in this section during the time period. Therefore, significant bed cover change can result from a combination of both local hydraulics and channel morphology as well as sediment supply variation.

It is possible to imagine the changes we observe in alluvial storage emerging due to different timescales and paths of sediment pulses traveling through the canyons. Sediment pulses can propagate through a reach by downstream translation or dispersing in place, with the possibility of both mechanisms occurring simultaneously (Sklar et al., 2009; Venditti et al., 2010b). Pulses at high transport stages are more likely to be translated, while at low stages are mostly dispersed (Humphries et al., 2012). In sand and gravel bedded rivers, sediment waves are commonly expressed as migrating dunes or bars, and transport rates can be inferred from their downstream movement (e.g. Gilbert and Murphy, 1914; Gomez and Church, 1989; Lisle et al., 2001; Madej and Ozaki, 1996). In contrast, in these canyon reaches sediment appears to move as large, discrete pulses that transfer relatively abruptly from one storage location to the next, suggesting a fundamentally different mode of sediment routing. Our results suggest that pulses disperse before becoming concentrated in wide and deep sections of the channel. This can explain how sediment is staged through the morphologies, with signals dispersed in reaches with fast and shallow flow (i.e. rapids) before reconcentrating in wide and deep reaches (e.g. pools at CPWs). This is observed at Tikwalus Rapid where the sediment pulse appears to disperse in Era 1 during the 2022 freshet before reconcentrating in the downstream wide section in Era 2 during the 2022-2023 annual cycle. We also see this at Yale Rapids and Lady Franklin Rock where pulses become concentrated in the widenings. This indicates that channel morphology may amplify sediment waves as pulses propagate downstream.

Due to the compounding complexity of sediment input and morphology influences on bed cover variation, it remains difficult to find discernible evidence of a single pulse propagating downstream through the canyon system. Changes in sediment supply are known to influence patch dynamics on the local scale with variations between individual patches (Nelson et al., 2009), and we observe this playing out at the reach scale through the Fraser Canyon. The grain size distribution of pulses and of the bed material have also been shown to influence the mobilization of sediment (Nelson et al., 2010; Venditti et al., 2010a, b). The exact role of grain size is yet to be explored in the Fraser Canyon and would contribute to understanding this dynamic. While the morphodynamics of a reach can provide clues to where sediment storage change is likely to occur, it remains challenging

https://doi.org/10.5194/egusphere-2026-819
Preprint. Discussion started: 11 March 2026


to predict whether storage will increase or decrease in specific locations due to staging and variations in the spacing and timing of sediment inputs.

## 5 Conclusion

High resolution repeat multibeam surveys were undertaken in the Lower Fraser Canyon to investigate the topographic variation in canyons where channels are constrained by bedrock on both sides for extended distances. Surveys encompassed CPWs, rapids, and overfalls, which are recurrent morphologies that create distinct flow structures in these reaches. Our observations show that bed elevation change during high flows can reach 15 m in large channels, and that areas of erosion and deposition are interspersed throughout canyons within the same flow period. We interpret the patterns of sediment storage to be driven by two signals: (1) local channel morphodynamics which control where storage occurs and (2) sediment staging of a high supply event that controls how storage changes. Additionally, we observe substantial changes in sediment storage without substantial changes in the storage footprint, indicating that bedrock exposure need not change with storage. CPWs tend to have a large continuous channel-spanning patch, rapids alternate between patches of erosion and deposition throughout their reach, and overfalls show almost no change. Sediment supplied from point sources (e.g. tributaries and mass movements) is passed through canyons causing variation in the magnitude and direction of storage change. As a result, storage change does not follow an annual cycle due to the influence of varied sediment input into each canyon through hillslope contributions or upstream erosion of bed cover. It remains difficult to predict how sediment storage will change in bedrock rivers due to the combined influence of channel morphology and complex sediment staging dynamics.

## Data Availability

Ross, C., Venditti, J. G., Larimer, J., and Viner, N.: Bathymetric Surveys of the Fraser Canyon (2021-2023), Federated Research Data Repository. https://doi.org/10.20383/103.01066, 2025

## Author Contribution

CBAR, JGV, JEL, and JCC are responsible for conceptualization; NV, JEL, JGV, and CBAR led the collection, cleaning, and processing of the multibeam data; CBAR visualized, analysed, and curated the data; CBAR wrote the manuscript draft; all authors reviewed and edited the manuscript; supervision was provided by JGV and JCC.

## Competing Interests

The authors declare that there is no conflict of interest.

https://doi.org/10.5194/egusphere-2026-819
Preprint. Discussion started: 11 March 2026


**Acknowledgements**

We thank the Nlaka'pamux and Yale First Nations for supporting our work and providing access to their traditional territories. LiDAR data were provided by the Hakai Institute Airborne Coastal Observatory and Brian Menounos of University of Northern British Columbia. Bathymetry processing was aided by Laurie Solkoski. We thank Darwin Baerg and the team at Rivertec for enabling our velocity and bathymetric mapping of bedrock canyons.

**Financial Support**

Funding supported by a British Columbia Salmon Restoration Innovation Fund (BCSRIF) grant to JGV and 9 others, as well as a Natural Science and Engineering Research Council of Canada (NSERC) Discovery Grant and Accelerator Supplement to JGV. The Hakai Institute provided in-kind support for geospatial data acquisition.

**References**

Alvarez, L. V. and Grams, P. E.: An Eddy-Resolving Numerical Model to Study Turbulent Flow, Sediment, and Bed Evolution Using Detached Eddy Simulation in a Lateral Separation Zone at the Field-Scale, J. Geophys. Res. Earth Surf., 126, e2021JF006149, https://doi.org/10.1029/2021JF006149, 2021.

Alvarez, L. V., Schmeeckle, M. W., and Grams, P. E.: A detached eddy simulation model for the study of lateral separation zones along a large canyon-bound river, J. Geophys. Res. Earth Surf., 122, 25–49, https://doi.org/10.1002/2016JF003895, 2017.

Baird, K.: Distribution and frequency of debris flows triggered by atmospheric rivers, Fraser Canyon, British Columbia, BSc, https://doi.org/10/Baird_Thesis_05242024.pdf, 2024.

Baker, V. R., Kochel, R. C., and Patton, P. C. (Eds.): Flood geomorphology, Wiley, ISBN 0-471-62558-2, 1988.

Beer, A. R., Turowski, J. M., and Kirchner, J. W.: Spatial patterns of erosion in a bedrock gorge, J. Geophys. Res. Earth Surf., 122, 191–214, https://doi.org/10.1002/2016JF003850, 2017.

Bretz, J. H.: The Dalles Type of River Channel, J. Geol., 32, 139–149, https://doi.org/10.1086/623074, 1924.

Buechel, M. E. H., Hodge, R. A., and Kenmare, S.: The influence of bedrock river morphology and alluvial cover on gravel entrainment: Part 1. Pivot angles and surface roughness, Earth Surf. Process. Landf., 47, 3361–3375, https://doi.org/10.1002/esp.5463, 2022.

Cao, Z. (E)., Venditti, J. G., and Li, T.: Experiments on Pool Formation in Bedrock Canyons, JGR Earth Surface, 127, e2021JF006456, https://doi.org/10.1029/2021JF006456, 2022.

Chatanantavet, P. and Parker, G.: Experimental study of bedrock channel alluviation under varied sediment supply and hydraulic conditions, Water Resour. Res., 44, W12446, https://doi.org/10.1029/2007WR006581, 2008.

https://doi.org/10.5194/egusphere-2026-819
Preprint. Discussion started: 11 March 2026


Cook, K. L., Turowski, J. M., and Hovius, N.: A demonstration of the importance of bedload transport for fluvial bedrock erosion and knickpoint propagation, Earth Surf. Process. Landf., 38, 683–695, https://doi.org/10.1002/esp.3313, 2013.

Cook, K. L., Turowski, J. M., and Hovius, N.: Width control on event-scale deposition and evacuation of sediment in bedrock-confined channels, Earth Surf. Process. Landf., 45, 3702–3713, https://doi.org/10.1002/esp.4993, 2020.

Curran, M., Steelquist, A. T., Larimer, J., Seagren, E., Li, T., Heathfield, D., Menounos, B., Clague, J. J., Church, M., and Venditti, J. G.: Structural control of bedrock river alignment and morphology in the Fraser Canyon, British Columbia, Canada, Earth Surf. Process. Landf., 48, 3381–3394, https://doi.org/10.1002/esp.5702, 2023.

DeLisle, C. and Yanites, B. J.: Rethinking Variability in Bedrock Rivers: Sensitivity of Hillslope Sediment Supply to Precipitation Events Modulates Bedrock Incision During Floods, J. Geophys. Res. Earth Surf., 128, e2023JF007148, https://doi.org/10.1029/2023JF007148, 2023.

Dolan, R., Howard, A., and Trimble, D.: Structural Control of the Rapids and Pools of the Colorado River in the Grand Canyon, Science, 202, 629–631, 1978.

Evenden, M. D.: Fish versus Power: An Environmental History of the Fraser River, Cambridge University Press, Cambridge, https://doi.org/10.1017/CBO9780511512032, 2004.

Finnegan, N. J., Sklar, L. S., and Fuller, T. K.: Interplay of sediment supply, river incision, and channel morphology revealed by the transient evolution of an experimental bedrock channel, J. Geophys. Res. Earth Surf., 112, F03S11, https://doi.org/10.1029/2006JF000569, 2007.

Fuller, T. K., Gran, K. B., Sklar, L. S., and Paola, C.: Lateral erosion in an experimental bedrock channel: The influence of bed roughness on erosion by bed load impacts, J. Geophys. Res. Earth Surf., 121, 1084–1105, https://doi.org/10.1002/2015JF003728, 2016.

Gasparini, N. M., Whipple, K. X., and Bras, R. L.: Predictions of steady state and transient landscape morphology using sediment-flux-dependent river incision models, J. Geophys. Res. Earth Surf., 112, F03S09, https://doi.org/10.1029/2006JF000567, 2007.

Gilbert, G. K. and Murphy, E. C.: The transportation of débris by running water, Journal of the Washington Academy of Sciences, 4, 154–158, 1914.

Gillett, N. P., Cannon, A. J., Malinina, E., Schnorbus, M., Anslow, F., Sun, Q., Kirchmeier-Young, M., Zwiers, F., Seiler, C., Zhang, X., Flato, G., Wan, H., Li, G., and Castellan, A.: Human influence on the 2021 British Columbia floods, Weather. Clim. Extrem., 36, 100441, https://doi.org/10.1016/j.wace.2022.100441, 2022.

Gomez, B. and Church, M.: An assessment of bed load sediment transport formulae for gravel bed rivers, Water Resour. Res., 25, 1161–1186, https://doi.org/10.1029/WR025i006p01161, 1989.

Goode, J. R. and Wohl, E.: Coarse sediment transport in a bedrock channel with complex bed topography, Water Resour. Res., 46, W11524, https://doi.org/10.1029/2009WR008135, 2010.

Graf, W. L.: Rapids in Canyon Rivers, J. Geol., 87, 533–551, 1979.

Grams, P. E., Schmidt, J. C., and Topping, D. J.: The rate and pattern of bed incision and bank adjustment on the Colorado River in Glen Canyon downstream from Glen Canyon Dam, 1956–2000, Geol. Soc. Am. Bull., 119, 556–575, https://doi.org/10.1130/B25969.1, 2007.

https://doi.org/10.5194/egusphere-2026-819
Preprint. Discussion started: 11 March 2026


Gran, K. B. and Czuba, J. A.: Sediment pulse evolution and the role of network structure, Geomorphology, 277, 17–30, https://doi.org/10.1016/j.geomorph.2015.12.015, 2017.

Hammack, L. and Wohl, E.: Debris-Fan Formation and Rapid Modification at Warm Springs Rapid, Yampa River, Colorado, J. Geol., 104, 729–740, 1996.

Hodge, R. A. and Buechel, M. E. H.: The influence of bedrock river morphology and alluvial cover on gravel entrainment. Part 2: Modelling critical shear stress, Earth Surf. Process. Landf., 47, 3348–3360, https://doi.org/10.1002/esp.5462, 2022.

Hodge, R. A. and Hoey, T. B.: A Froude-scaled model of a bedrock-alluvial channel reach: 2. Sediment cover, J. Geophys. Res. Earth Surf., 121, 1597–1618, https://doi.org/10.1002/2015JF003709, 2016.

Hodge, R. A., Hoey, T. B., and Sklar, L. S.: Bed load transport in bedrock rivers: The role of sediment cover in grain entrainment, translation, and deposition, J. Geophys. Res. Earth Surf., 116, F04028, https://doi.org/10.1029/2011JF002032, 2011.

Humphries, R., Venditti, J. G., Sklar, L. S., and Wooster, J. K.: Experimental evidence for the effect of hydrographs on sediment pulse dynamics in gravel-bedded rivers, Water Resour. Res., 48, W01533, https://doi.org/10.1029/2011WR010419, 2012.

Hunt, B., Venditti, J. G., and Kwoll, E.: Experiments on the morphological controls of velocity inversions in bedrock canyons, Earth Surf. Process. Landf., 43, 654–668, https://doi.org/10.1002/esp.4274, 2018.

Hurson, M., Venditti, J. G., Rennie, C. D., Kwoll, E., Fairweather, K., Haught, D. R. W., Kusack, K. M., and Church, M.: Amplification of Plunging Flows in Bedrock Canyons, Geophys. Res. Lett., 49, e2022GL098487, https://doi.org/10.1029/2022GL098487, 2022.

Hurson, M., Venditti, J. G., Rennie, C. D., Kwoll, E., Fairweather, K., Haught, D., Ansari, S., Kusack, K. M., and Church, M.: The Abundance and Persistence of Plunging Flows in Bedrock Canyons, J. Geophys. Res. Earth Surf., 130, e2024JF007807, https://doi.org/10.1029/2024JF007807, 2025.

Hurson, M., Larimer, J., Ross, C., and Venditti, J. G.: The Diversity of Flow Structures and Dynamics in Bedrock Rivers, in review.

Inoue, T., Izumi, N., Shimizu, Y., and Parker, G.: Interaction among alluvial cover, bed roughness, and incision rate in purely bedrock and alluvial-bedrock channel, J. Geophys. Res. Earth Surf., 119, 2123–2146, https://doi.org/10.1002/2014JF003133, 2014.

Johnson, J. P. L.: A surface roughness model for predicting alluvial cover and bed load transport rate in bedrock channels, J. Geophys. Res. Earth Surf., 119, 2147–2173, https://doi.org/10.1002/2013JF003000, 2014.

Johnson, J. P. L. and Whipple, K. X.: Evaluating the controls of shear stress, sediment supply, alluvial cover, and channel morphology on experimental bedrock incision rate, J. Geophys. Res. Earth Surf., 115, F02018, https://doi.org/10.1029/2009JF001335, 2010.

Kieffer, S. W.: The 1983 Hydraulic Jump in Crystal Rapid: Implications for River-Running and Geomorphic Evolution in the Grand Canyon, J. Geol., 93, 385–406, https://doi.org/10.1086/628962, 1985.

Kieffer, S. W.: Hydraulic maps of major rapids of the Colorado River, U.S. Geol. Surv. Misc, Invest. Maps 1897 A-J., 1988.

https://doi.org/10.5194/egusphere-2026-819
Preprint. Discussion started: 11 March 2026


Kieffer, S. W.: Geologic nozzles, Rev. Geophys., 27, 3–38, https://doi.org/10.1029/RG027i001p00003, 1989.

Kuo, C.-W. and Brierley, G.: The influence of landscape connectivity and landslide dynamics upon channel adjustments and sediment flux in the Liwu Basin, Taiwan, Earth Surf. Process. Landf., 39, 2038–2055, https://doi.org/10.1002/esp.3598, 2014.

Kusack, K. M., Li, T., and Venditti, J. G.: Experiments on Constriction-Pool-Widening Morphology in Bedrock Canyons, J. Geophys. Res. Earth Surf., 129, e2024JF007808, https://doi.org/10.1029/2024JF007808, 2024.

Lague, D.: Reduction of long-term bedrock incision efficiency by short-term alluvial cover intermittency, J. Geophys. Res. Earth Surf., 115, F02011, https://doi.org/10.1029/2008JF001210, 2010.

Lamb, M. P., Dietrich, W. E., and Sklar, L. S.: A model for fluvial bedrock incision by impacting suspended and bed load sediment, J. Geophys. Res. Earth Surf., 113, F03025, https://doi.org/10.1029/2007JF000915, 2008.

Lamb, M. P., Finnegan, N. J., Scheingross, J. S., and Sklar, L. S.: New insights into the mechanics of fluvial bedrock erosion through flume experiments and theory, Geomorphology, 244, 33–55, https://doi.org/10.1016/j.geomorph.2015.03.003, 2015.

Larimer, J. E., Yager, E. M., Yanites, B. J., and Witsil, A. J. C.: Flume Experiments on the Erosive Energy of Bed Load Impacts on Rough and Planar Beds, J. Geophys. Res. Earth Surf., 126, e2020JF005834, https://doi.org/10.1029/2020JF005834, 2021.

Larsen, I. J. and Lamb, M. P.: Progressive incision of the Channeled Scablands by outburst floods, Nature, 538, 229–232, https://doi.org/10.1038/nature19817, 2016.

Larsen, I. J., Schmidt, J. C., and Martin, J. A.: Debris-fan reworking during low-magnitude floods in the Green River canyons of the eastern Uinta Mountains, Colorado and Utah, Geology, 32, 309–312, https://doi.org/10.1130/G20235.1, 2004.

Leopold, L. B.: The rapids and the pool: Grand Canyon, Professional Paper, U.S. Government Printing Office, https://doi.org/10.3133/pp669D, 1969.

Li, T., Fuller, T. K., Sklar, L. S., Gran, K. B., and Venditti, J. G.: A Mechanistic Model for Lateral Erosion of Bedrock Channel Banks by Bedload Particle Impacts, J. Geophys. Res. Earth Surf., 125, e2019JF005509, https://doi.org/10.1029/2019JF005509, 2020.

Li, T., Venditti, J. G., and Sklar, L. S.: An Analytical Model for Lateral Erosion From Saltating Bedload Particle Impacts, J. Geophys. Res. Earth Surf., 126, e2020JF006061, https://doi.org/10.1029/2020JF006061, 2021.

Li, T., Venditti, J. G., Rennie, C. D., and Nelson, P. A.: Bed and Bank Stress Partitioning in Bedrock Rivers, J. Geophys. Res. Earth Surf., 127, e2021JF006360, https://doi.org/10.1029/2021JF006360, 2022.

Li, T., Venditti, J. G., and Sklar, L. S.: Steady-State Bedrock Channel Width, Geophys. Res. Lett., 50, e2023GL105344, https://doi.org/10.1029/2023GL105344, 2023.

Lisle, T. E., Cui, Y., Parker, G., Pizzuto, J. E., and Dodd, A. M.: The dominance of dispersion in the evolution of bed material waves in gravel-bed rivers, Earth Surf. Process. Landf., 26, 1409–1420, https://doi.org/10.1002/esp.300, 2001.

Madej, M. A. and Ozaki, V.: Channel Response to Sediment Wave Propagation and Movement, Redwood Creek, California, Usa, Earth Surf. Process. Landf., 21, 911–927, https://doi.org/10.1002/(SICI)1096-9837(199610)21:10%3C911::AID-ESP621%3E3.0.CO;2-1, 1996.

https://doi.org/10.5194/egusphere-2026-819
Preprint. Discussion started: 11 March 2026


Magirl, C. S., Gartner, J. W., Smart, G. M., and Webb, R. H.: Water velocity and the nature of critical flow in large rapids on the Colorado River, Utah, Water Resour. Res., 45, W05427, https://doi.org/10.1029/2009WR007731, 2009.

Mueller, E. R., Grams, P. E., Hazel, J. E., and Schmidt, J. C.: Variability in eddy sandbar dynamics during two decades of controlled flooding of the Colorado River in the Grand Canyon, Sedimentary Geology, 363, 181–199, https://doi.org/10.1016/j.sedgeo.2017.11.007, 2018.

Nelson, P. A., Venditti, J. G., Dietrich, W. E., Kirchner, J. W., Ikeda, H., Iseya, F., and Sklar, L. S.: Response of bed surface patchiness to reductions in sediment supply, J. Geophys. Res. Earth Surf., 114, F02005, https://doi.org/10.1029/2008JF001144, 2009.

Nelson, P. A., Dietrich, W. E., and Venditti, J. G.: Bed topography and the development of forced bed surface patches, J. Geophys. Res. Earth Surf., 115, F04024, https://doi.org/10.1029/2010JF001747, 2010.

Ouimet, W. B., Whipple, K. X., Crosby, B. T., Johnson, J. P., and Schildgen, T. F.: Epigenetic gorges in fluvial landscapes, Earth Surf. Process. Landf., 33, 1993–2009, https://doi.org/10.1002/esp.1650, 2008.

Rennie, C. D., Church, M., and Venditti, J. G.: Rock Control of River Geometry: The Fraser Canyons, J. Geophys. Res. Earth Surf., 123, 1860–1878, https://doi.org/10.1029/2017JF004458, 2018.

Scheingross, J. S. and Lamb, M. P.: Sediment transport through self-adjusting, bedrock-walled waterfall plunge pools, J. Geophys. Res. Earth Surf., 121, 939–963, https://doi.org/10.1002/2015JF003620, 2016.

Scheingross, J. S., Brun, F., Lo, D. Y., Omerdin, K., and Lamb, M. P.: Experimental evidence for fluvial bedrock incision by suspended and bedload sediment, Geology, 42, 523–526, https://doi.org/10.1130/G35432.1, 2014.

Scheingross, J. S., Lo, D. Y., and Lamb, M. P.: Self-formed waterfall plunge pools in homogeneous rock, Geophys. Res. Lett., 44, 200–208, https://doi.org/10.1002/2016GL071730, 2017.

Schmidt, J. C.: Recirculating Flow and Sedimentation in the Colorado River in Grand Canyon, Arizona, J. Geol., 98, 709–724, https://doi.org/10.1086/629435, 1990.

Schmidt, J. C. and Rubin, D. M.: Regulated Streamflow, Fine-Grained Deposits, and Effective Discharge in Canyons with Abundant Debris Fans, in: Natural and Anthropogenic Influences in Fluvial Geomorphology, American Geophysical Union, 177–195, https://doi.org/10.1029/GM089p0177, 1995.

Sepúlveda, S. A., Ward, B. C., Cosman, S. B., and Jacobs, R.: Preliminary investigations of ground failures triggered during the mid-November 2021 atmospheric river event along the southwestern British Columbia highway corridors, Can. Geotech. J., 60, 580–586, https://doi.org/10.1139/cgj-2022-0093, 2023.

Shobe, C. M., Tucker, G. E., and Barnhart, K. R.: The SPACE 1.0 model: a Landlab component for 2-D calculation of sediment transport, bedrock erosion, and landscape evolution, Geoscientific Model Development, 10, 4577–4604, https://doi.org/10.5194/gmd-10-4577-2017, 2017.

Sklar, L. and Dietrich, W. E.: River Longitudinal Profiles and Bedrock Incision Models: Stream Power and the Influence of Sediment Supply, in: Rivers Over Rock: Fluvial Processes in Bedrock Channels, American Geophysical Union, 237–260, https://doi.org/10.1029/GM107p0237, 1998.

Sklar, L. S.: Grain Size in Landscapes, Annu. Rev. Earth Planet. Sci., 52, 663–692, https://doi.org/10.1146/annurev-earth-052623-075856, 2024.

https://doi.org/10.5194/egusphere-2026-819
Preprint. Discussion started: 11 March 2026


Sklar, L. S. and Dietrich, W. E.: Sediment and rock strength controls on river incision into bedrock, Geology, 29, 1087–1090, https://doi.org/10.1130/0091-7613(2001)029%3C1087:SARSCO%3E2.0.CO;2, 2001.

Sklar, L. S. and Dietrich, W. E.: A mechanistic model for river incision into bedrock by saltating bed load, Water Resour. Res., 40, W06301, https://doi.org/10.1029/2003WR002496, 2004.

Sklar, L. S., Fadde, J., Venditti, J. G., Nelson, P., Wydzga, M. A., Cui, Y., and Dietrich, W. E.: Translation and dispersion of sediment pulses in flume experiments simulating gravel augmentation below dams, Water Resour. Res., 45, W08439, https://doi.org/10.1029/2008WR007346, 2009.

Turowski, J. M., Lague, D., and Hovius, N.: Cover effect in bedrock abrasion: A new derivation and its implications for the modeling of bedrock channel morphology, J. Geophys. Res. Earth Surf., 112, F04006, https://doi.org/10.1029/2006JF000697, 2007.

Turowski, J. M., Hovius, N., Meng-Long, H., Lague, D., and Men-Chiang, C.: Distribution of erosion across bedrock channels, Earth Surf. Process. Landf., 33, 353–363, https://doi.org/10.1002/esp.1559, 2008.

Turowski, J. M., Badoux, A., Leuzinger, J., and Hegglin, R.: Large floods, alluvial overprint, and bedrock erosion, Earth Surf. Process. Landf., 38, 947–958, https://doi.org/10.1002/esp.3341, 2013.

Venditti, J. G.: Morphodynamics of Bedrock Rivers, Annu. Rev. Earth Planet. Sci., 54, 8.1-8.29, https://doi.org/10.1146/annurev-earth-040523-023051, 2026.

Venditti, J. G., Dietrich, W. E., Nelson, P. A., Wydzga, M. A., Fadde, J., and Sklar, L.: Effect of sediment pulse grain size on sediment transport rates and bed mobility in gravel bed rivers, J. Geophys. Res. Earth Surf., 115, F03039, https://doi.org/10.1029/2009JF001418, 2010a.

Venditti, J. G., Dietrich, W. E., Nelson, P. A., Wydzga, M. A., Fadde, J., and Sklar, L.: Mobilization of coarse surface layers in gravel-bedded rivers by finer gravel bed load, Water Resour. Res., 46, W07506, https://doi.org/10.1029/2009WR008329, 2010b.

Venditti, J. G., Rennie, C. D., Bomhof, J., Bradley, R. W., Little, M., and Church, M.: Flow in bedrock canyons, Nature, 513, 534–537, https://doi.org/10.1038/nature13779, 2014.

Venditti, J. G., Fairweather, K., Kwoll, E., Wong, M., Lin, C.-Y. M., Rennie, C. D., and Church, M.: Atlas of the Fraser Canyons. River Dynamics Laboratory, Simon Fraser University, FRDR [dataset], https://doi.org/10.20383/101.0276, 2020a.

Venditti, J. G., Li, T., Deal, E., Dingle, E., and Church, M.: Struggles with stream power: Connecting theory across scales, Geomorphology, 366, 106817, https://doi.org/10.1016/j.geomorph.2019.07.004, 2020b.

Webb, R. H., Pringle, P. T., Reneau, S. L., and Rink, G. R.: Monument Creek debris flow, 1984: Implications for formation of rapids on the Colorado River in Grand Canyon National Park, Geology, 16, 50–54, https://doi.org/10.1130/0091-7613(1988)016%3C0050:MCDFIF%3E2.3.CO;2, 1988.

Whipple, K. X. and Meade, B. J.: Controls on the strength of coupling among climate, erosion, and deformation in two-sided, frictional orogenic wedges at steady state, J. Geophys. Res. Earth Surf., 109, F01011, https://doi.org/10.1029/2003JF000019, 2004.

Whipple, K. X., DiBiase, R. A., and Crosby, B. T.: 9.28 Bedrock Rivers, in: Treatise on Geomorphology, edited by: Shroder, J. F., Academic Press, San Diego, 550–573, https://doi.org/10.1016/B978-0-12-374739-6.00254-2, 2013.

https://doi.org/10.5194/egusphere-2026-819
Preprint. Discussion started: 11 March 2026


Wohl, E. E.: Bedrock Channel Morphology in Relation to Erosional Processes, in: Rivers Over Rock: Fluvial Processes in Bedrock Channels, edited by: Tinkler, K. J., American Geophysical Union, 133–151, https://doi.org/10.1029/GM107p0133, 1998.

Wohl, E. E.: Particle dynamics: The continuum of bedrock to alluvial river segments, Geomorphology, 241, 192–208, https://doi.org/10.1016/j.geomorph.2015.04.014, 2015.

Wohl, E. E. and Merritt, D. M.: Bedrock channel morphology, Geol. Soc. Am. Bull., 113, 1205–1212, https://doi-org.proxy.lib.sfu.ca/10.1130/0016-7606(2001)113%3C1205:BCM%3E2.0.CO;2, 2001.

Wright, M., Venditti, J. G., Li, T., Hurson, M., Chartrand, S., Rennie, C., and Church, M.: Covariation in width and depth in bedrock rivers, Earth Surf. Process. Landf., 47, 1570–1582, https://doi.org/10.1002/esp.5335, 2022.

Wright, M. J., Hurson, M., Robinson, K. A., Patterson, D. A., and Venditti, J. G.: A typology of potential hydraulic barriers to adult salmon migration in a bedrock river, Can. J. Fish. Aquat. Sci., 83, 1-19, https://doi.org/10.1139/cjfas-2024-0100, 2024.

Yanites, B. J.: The Dynamics of Channel Slope, Width, and Sediment in Actively Eroding Bedrock River Systems, J. Geophys. Res. Earth Surf., 123, 1504–1527, https://doi.org/10.1029/2017JF004405, 2018.

Zhang, L., Parker, G., Stark, C. P., Inoue, T., Viparelli, E., Fu, X., and Izumi, N.: Macro-roughness model of bedrock–alluvial river morphodynamics, Earth Surf. Dyn., 3, 113–138, https://doi.org/10.5194/esurf-3-113-2015, 2015.